A Novel Technique to Irradiate Surgical Scars using Dynamic Electron Arc Radiotherapy

By

Johannes Addido

Graduate Program in Medical Physics
Duke Kunshan University and Duke University

Date: _____

Approved:

_____
Qiuwen Wu, Supervisor

_____
David Huang

_____
Justus Adamson

Thesis submitted in partial fulfillment of
the requirements for the degree of
Master of Science in the Medical Physics Program
Duke Kunshan University and Duke University

2017

ABSTRACT

A Novel Technique to Irradiate Surgical Scars using Dynamic Electron Arc Radiotherapy

By

Johannes Addido

Graduate Program in Medical Physics
Duke Kunshan University and Duke University

Date: _____

Approved:

_____
Qiuwen Wu, Supervisor

_____
David Huang

_____
Justus Adamson

An abstract of a thesis submitted in partial
fulfillment of the requirements for the degree
of Master of Science in the Medical Physics Program
Duke Kunshan University and Duke University

2017

Abstract

Purpose: The usage of conformal electron beam therapy techniques in treating superficial tumors on uneven surfaces has often lead to undesired outcomes such as non-uniform dose inside the target and a wide penumbra at boundary of the target. The dynamic electron arc radiotherapy (DEAR) technique has been demonstrated to improve dose distribution and minimize penumbra. The aim of this study is to investigate the feasibility and the accuracy of DEAR technique in irradiating surgical scars.

Method: 3D scar coordinates, a series of connected points along a line extracted from CT images were used. A treatment plan was designed to irradiate the scar with a uniform dose. An algorithm was developed to produce a DEAR plan consisting of control points (CP) corresponding to various positions along machine mechanical axes as a function of MU. Varian's Spreadsheet based Automatic Generator (SAGE) software was used to verify and simulate the treatment and also to generate the plan in XML format. XML file was loaded on a TrueBeam Linac in research mode for delivery. The technique was demonstrated in i) a straight line scar on the surface of a solid water phantom and ii) curved scar on the surface of a cylindrical phantom. Energy used was 6MeV and a 6x6 cm^2 applicator fitted with a 3x3 cm^2 cutout. Dose at the surface and dmax were measured with Gafchromic film. Dose profiles calculated from the Eclipse eMC and Virtual Linac Monte Carlo tool were compared to film dose measurement.

Results: The dose profile analysis show that the TrueBeam Linac can deliver the designed plans for both straight line and arc scars to a high degree of accuracy. The root mean square error (RMSE) value for the line scar is approximately 0.0035^0 Gantry angle and it is 0.0349 for the arc scar. This is due to the fact that in the straight line delivery the gantry angle is static so it has a higher degree of agreement than in the arc delivery. RMSE values for the straight line scar has an overall high degree of agreement compared to the arc scar because the arc scar delivery has more mechanical axes motion during delivery.

Conclusion: The DEAR technique can be used to treat various line targets (scars) i.e. straight or curved lines, to a high degree of accuracy. This treatment modality can help reinvigorate electron therapy and make it a clinically viable treatment option.

Dedication

To

Edwin Teye Addido, Sarah Asare, Naabi, Nene

Thank you.

Contents

List of Tables

List of Figures

Acknowledgements

I would like to thank my thesis advisor, Dr. Qiuwen Wu, foe helping me to complete this project through his guidance, knowledge and enormous patience. I would also like to thank Dr. David Huang and Dr. Justus Adamson for serving on my committee. To Dr. James Bowsher and Dr. Fang-Fang Yin, thank you for your faith in me, it carried me to the finish line. I am eternally grateful to Duke Kunshan University and Duke University for admitting me and granting me the opportunity to pursue my graduate studies on their world class campuses. I thank Dr. Patrick Moreton for all the help in securing financial support for my studies and am profoundly grateful to the Guo Tingting Scholarship. Thank you also to Kaimei Luo for all the support and effort you put into making my graduate studies a success. To Dr. Deedra McClearn, Dr. Sharon Wang, Dr. Anna Rodrigues, Danni Shen and Edith Allen thank you for all of the help. To my siblings who have endured the last two years hoping and praying for my success, thanks for your patience and support. Finally, to Rosemary Gidiglo, I offer my great appreciation for all the love and silent prayers for my success.

1. Introduction

1.1 Electron beam therapy

Electrons in the 6 to 20 MeV energy range have been used clinically in treating tumors that are less than 5cm deep for decades. The increase in the commercial development of linear accelerators has greatly contributed to the clinical expertise acquired in using electron beams to treat tumors[1]. Electron beam therapy as a treatment technique has not undergone rapid transformations like photon therapy even though treatment machines with multiple energies are very common in most radiotherapy centers[2]. Radiotherapy has become synonymous with photon beam therapy due to the major technological advancements this modality has enjoyed in recent decades. The increased clinical research directed at overcoming the challenges and limitations that photon therapy faced has been to the detriment of the development of electron therapy and has contributed to its relative anonymity in the radiotherapy treatment suite[3].

1.2 Generating electron and photon beams

Modern linear accelerators can generate multiple electron and photon beam energies; hence electron beams are readily available. The electron beam energies available on these machines are 6, 9, 12, 16, 20, and 22 MeV. The photon beam energies that these Linacs can generate are 6, 10, and 15 MV. The electrons that exit the window of the accelerator tube are narrow with a diameter of about 3 mm. These high speed

electrons in the Linac head can either be incident on a high-Z tungsten target or instead strike an electron scattering foil. If the former happens, a bremstrahlung interaction occurs and the electron beams are converted into X-ray photons. The latter scenario will lead to the spreading of the electron beam to get uniform electron fluence across the field[1]. Figure 1 shows a Linac treatment head schematically demonstrating how electron and photon beams are generated.

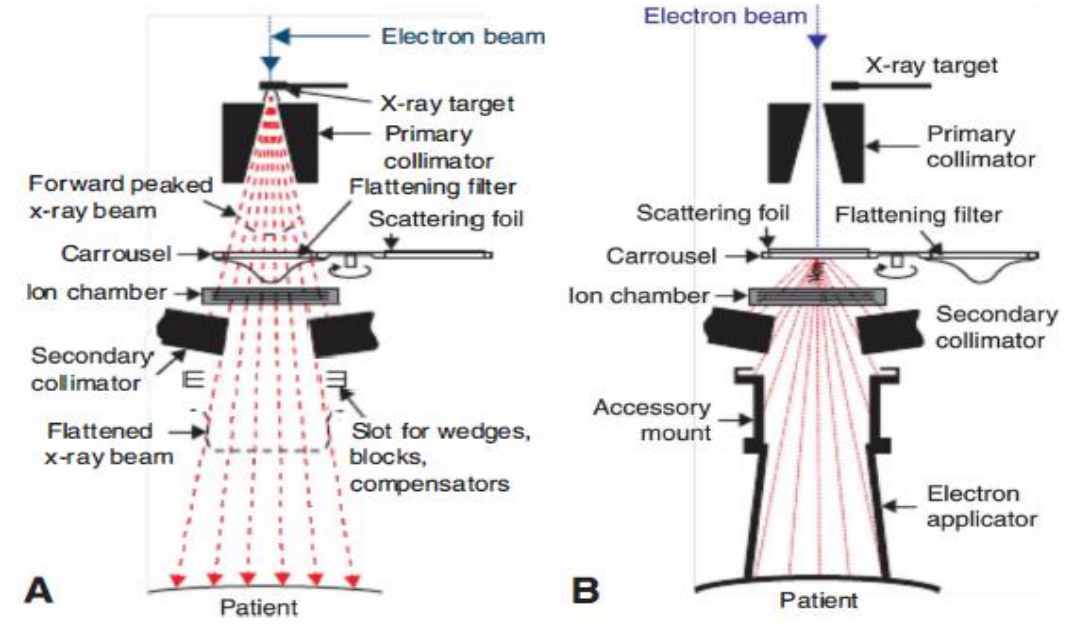

Figure 1: Schematic diagrams showing Linac heads in (A) Photon therapy mode. (B) Electron therapy mode. *(From Khan's the Physics of radiation therapy fifth edition)*

The diagrams in figure 1show some fundamental differences between electron beams and photons from a mechanical perspective. The x-ray target is right in the path of the electron beams in (A), thus generating x-rays whiles in (B) it is removed, hence the production of an electron beam. In diagram (A) a flattening filter is placed in the

carrousel and in (B) a scattering foil is in the carrousel. The flattening filter in the path of the x-ray beam which is mostly made of lead creates uniform beam intensity across the field, whereas the purpose of the scattering foil is to broaden the narrow pencil beam of electrons incident on it[1][4]. Previous studies have shown that electrons scatter easily in air and this has an adverse effect on output. It is therefore important to prevent this means that electron beam collimation must be done close to the patient's skin surface. The electron applicator or cone helps to achieve this objective. It serves as a tertiary collimation system to narrow the beam penumbra[1].

1.3 Interactions of electron and photon beams in tissue equivalent media

When high energy electron and photon beams interact with a tissue equivalent medium like water, the energy deposited in the medium as a function of depth is represented by the percent depth dose curve[1][3]. Figure 2 and figure 3 below show percent depth dose (PDD) curves in water for electron and photon beams.

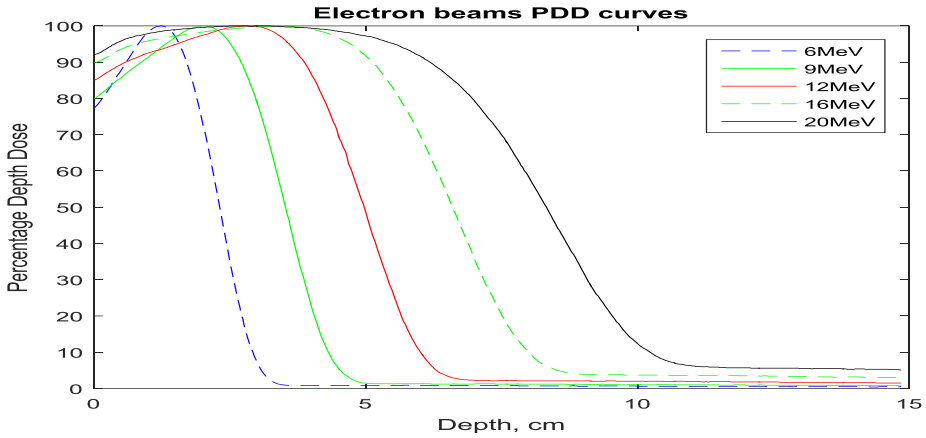

Figure 2: PDD curves for multiple electron beams in water. Curves plotted using data obtained in commissioning TrueBeam Linac at DUMC.

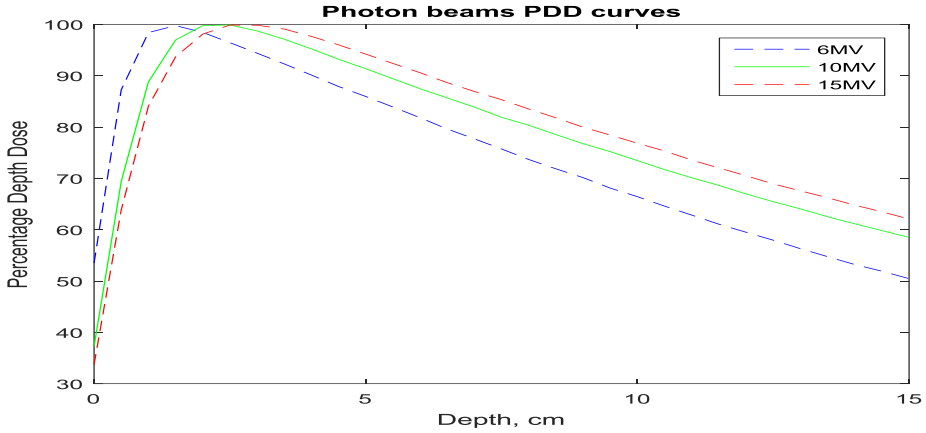

Figure 3: PDD curves for multiple photon beams in water. Curves plotted using data obtained in commissioning TrueBeam Linac at DUMC.

The electron PDD curves in figure 2 show a steep build-up region with a peak at the dmax. A sharp fall-off region precedes the x-ray contamination tail[3]. The depth of maximum dose for the electron beams is relatively shallow and this indicates a high surface dose. This feature makes electron beams more suitable for treating shallow tumors.

The photon PDD curves in figure 3 show a relatively gentle dose build-up hence has a low surface dose compared to electron beams. The surface dose of photon beams decreases with increase in beam energy; this characterizes the skin sparing effect that makes photons less suitable for treating superficial tumors. At the depths that superficial tumors are treated, photons have a comparatively high exit dose and this can cause normal tissue toxicity[5][6].

1.4 Electron beam treatment sites

Electron beams are most suitable for treating superficial tumors and disease that lie few centimeters below a patient's skin[7][8]. The irradiation of these cancers at shallow depths minimizes the radiation dose to the underlying normal tissues and organs[4][9]. Sites that are commonly treated with electron therapy are skin, head and neck, scalp, extremities, breast and chest wall. The lung and heart tissues are spared when the chest wall is treated with electron beams while covering the target adequately than treating these sites with tangential photon beams[3][10]. Lung toxicity, such as lung pneumonitis which is a common side effect with photon therapy is minimized when the site is treated with electron beams[7][11][12]. When the head and neck region, skin or lip of a patient is treated with electron therapy, the mucous membrane which lines the digestive system from the mouth to the anus is largely spared from radiation toxicity[6][13][14][15].

The failure of electron beam therapy to become a major treatment modality clinically can be attributed to some of the problems associated with conventional electron therapy. A single electron beam of fixed energy is normally used in treating targets on a flat surface with favourable outcomes but its treatment outcomes are not good on curved surfaces[4]. A non-uniform dose inside the target and a wide penumbra at the target boundary occurs when a single electron beam is used in treating a target on a curved surface. The use of multiple static abutting beams often leads to hot and or cold spots at the beam junction[2].

1.5 Conformal electron therapy

Conformal electron therapy is the use of one or more electron beams for containing the target volume in the 90% isodose line, achieving a high dose homogeneity i.e. 90-100% and minimizing dose to critical structures and normal tissues[4]. Treating a large target on a curved surface with a single large electron beam will produce dose inhomogeneity inside the target and wide penumbra at the target boundary. Multiple static abutting beams often produce hot and/or cold spots at the beam junction region[2][3]. Thus it became necessary to seek ways of improving this therapeutic technique (conformal electron therapy) for optimal clinical utilization. The treatment modalities developed to achieve the above aim are numerous but this paper

will look at electron arc therapy (EAT), modulated electron radiation therapy (MERT) and scanning electron beam.

Electron Arc Therapy (EAT): This technique is best used in treating shallow (less than 5cm depth) tumors on curved surfaces such as chest wall, ribs, arms, thighs and legs[2][3][16][17][18][19][20]. The Electron arc therapy technique has been used clinically to treat tumors on the chest wall since it was introduced about three decades ago. EAT spares the underlying lung and heart tissues, a quality that makes it more clinically advantageous compared to tangential photon beams[2][21][22][23]. EAT planning and delivery is done in such a way that the isocenter is inside the patient. The SSD is much shorter than the standard 100cm hence a shorter electron applicator/cone is used to avoid collision with the patient[3][24]. Secondary and modified tertiary collimators are used to maintain beam penumbra. In order to protect areas outside the target volume, shields or molds are used to improve penumbra. Merits of EAT include producing homogeneous dose distributions and solving dose heterogeneities related to static abutting fields. The drawbacks of this technique are the challenges of manufacturing patient-specific casts and customized bolus. It also requires time consuming planning and an intensive physics support program which discourages most treatment centers from implementing it[2].

Modulated Electron Radiation Therapy (MERT): MERT is a conformal technique which modulates electron energy and intensity[25][26][27][28][29][20][30].

This technique works to achieve beam axis dose conformity by modulating the electron beam energy. Intensity modulation and lateral dose constriction are also achieved by using electron multi-leaf collimators (eMLC), cutouts or scanned beam[2][5][31]. Though the MERT technique does not require eMLCs, it makes it more convenient for clinical implementation and the commercial availability of eMLCs will hasten the clinical adoption of this technique.

Scanning electron beam: State of the art linear accelerators can produce electron beams with the required beam width desired for clinical use by employing the scanning electron beam technique. These Linacs are designed without a scattering foil in their treatment heads. The electron beams are deflected using two computer controlled magnets to deflect the pencil beam in two orthogonal planes. This helps to generate a moving electron beam across the field[3][32]. The scanning beam technique's advantage over the more conventional mode of generating electron beams is that it prevents bremsstrahlung contamination. Bremsstrahlung contamination of an electron beam can come from the collimators, ionization chambers, electron applicators and air but the scattering foil is the biggest contributor[33][34]. The complex electronic system needed to steer the electron beam, a fundamental component of this technique, has also proven to be its biggest drawback. The fatal cases of radiation over-dosed patients due to electronic system failures have led to the termination of this treatment technique[3][35].

1.6 Feasibility of using dynamic electron arc radiotherapy for scar irradiation

This research work seeks to demonstrate the feasibility of using the dynamic electron arc radiotherapy (DEAR) technique to irradiate surgical scars on flat and curved surfaces.

The DEAR technique is a novel conformal electron beam treatment modality. Radiation is delivered whiles the gantry and couch move simultaneously i.e. in arc mode with a standard electron applicator of length 95 cm fixed to the treatment head. The simultaneous motion of the gantry and couch helps to avoid collisions between patient and Linac head whiles the patient is on the couch. In this technique small apertures are utilized to produce desired dose distributions even though large apertures can be employed as well[3][2].

The feasibility of delivering the DEAR technique and its potential to improve dose distributions has already been demonstrated by Rodrigues et al[2][3] using simple cylindrical phantoms. The scars to be treated vary in shape and size; this makes it very difficult to treat with EAT, which requires the manufacturing of patient specific casts. EAT requires casts and customized bolus to balance the uneven target thickness. This is something that DEAR does not require because the delivery uses standard cones fitted with cutouts in place of patient specific cast. Planning treatments for DEAR is less

intensive and does not need a demanding physics support program. This reduces the degree of uncertainties when planning treatments for scars on curved surfaces.

DEAR does not need photon MLC or an eMLC like MERT; the former contributes to scatter and the latter is not readily available. This means that DEAR offers a level of simplicity that makes it comparatively easy to implement, something that MERT and the scanning beam technique lack. The DEAR technique can be implemented with hardware and software that are already available in a standard radiotherapy unit hence minimal or no extra cost is incurred.

The advantages that DEAR has over other standard electron therapy modalities such as MERT and EAT are well enumerated[2][3]. DEAR delivery is always orthogonal to the curved skin surface. This is something that cannot be done with MERT and makes DEAR very suitable for curved surfaces because of the even dose distribution that is produced during delivery. The mechanical capabilities of DEAR are better than those of MERT and EAT. The mechanical motion of the Linac axes is controlled by the computer system, which has high temporal response and can also hold the beam in the middle of delivery to avert undue radiation exposure to the patient. The recording of trajectory log files gives DEAR an upper hand when it comes to quality control. The recorded trajectories allows the planner to reconstruct treatment delivery and make it better than a previous delivery, this implies the DEAR technique can offer optimum delivery in most cases. The use of XML created plans means that the synchronous motion of

machine axes is predetermined. DEAR is not prone to the issues of safety during delivery that affect other treatment techniques which employ simultaneous gantry and couch motion. The XML file contains preset/programmed trajectories that are based on patient geometry and scar geometry thus, the movement of mechanical axes always follows a fixed pattern.

This research will investigate the DEAR technique's feasibility in terms of deliverability and dose homogeneity with regards to irradiating surgical scars on flat and curved surfaces. This investigation will be done on the TrueBeam Linac (Varian Medical Systems, Inc., Palo Alto, CA) in Research mode. Since the DEAR technique is not yet clinically approved to be used on both human and animal subjects, it can only be delivered in research mode.

2. Methods and Materials

Given 3D scar coordinates extracted from CT images of scars similar to real patients' scars, parameters such as gantry angle and couch motions, i.e. vertical, lateral and longitudinal must be determined to help create a treatment plan. The plan was used to generate a file in XML format that can be delivered on a TrueBeam Linac (Varian Medical Systems, Inc., Palo Alto, CA) in research mode.

When creating a treatment plan for irradiating scars using the DEAR technique certain parameters are kept constant. In the case of this particular project the following parameters were kept constant i.e. remain the same for all the treatment plans developed for all the given scars. They are:

a. Electron beam energy
b. Applicator
c. Cutout
d. Couch rotation
e. Dose rate

In the case of developing treatment plans for the scars to be irradiated using the DEAR technique, the following parameters changed with respect to the size and shape of the 3D scars. They are:

a. Gantry angle
b. Couch lateral, vertical and longitudinal positions
c. MU
d. Collimator angle

Generating Gantry angle

When irradiating a scar using the DEAR technique the gantry angle or position must always be tangential to the point on the scar it is irradiating. With the given scar coordinates, i.e. the x and y coordinates the gantry angle relative to a particular point on the scar was determined by using the equations below.

$$K_i = (y_{i+1} - y_{i-1})/(x_{i+1} - x_{i-1}) \qquad \text{Eqn. 1}$$

Where K_i is the gradient of the line joining the two points (i-1) and (i+1) on the x and y planes.

$$\acute{K} = \frac{-1}{K_i} = \tan\theta \qquad \text{Eqn. 2}$$

Where K` is the slope of the line corresponding to the gantry angle, θ for index i.

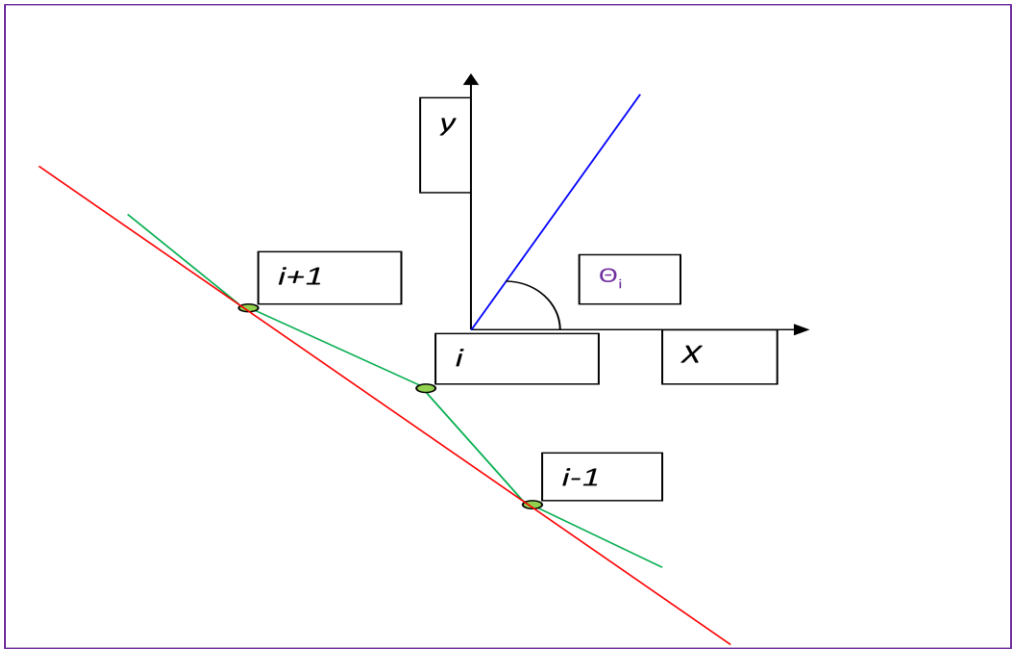

Figure 4: Determining gantry angle at index i. Gantry must be perpendicular to index i, indicated with the blue line.

The total gantry angle for the complete irradiation of the scar is the accumulation of all the angles corresponding to each coordinate point on the scar.

Generating Couch positions

The Couch must change positions vertically, laterally and longitudinally in order to completely irradiate the curved or arc line scar. With the scar coordinates already given, initial positions must be chosen so that the SSD is always 100cm irrespective of the couch positions or gantry angle. Initial couch vertical, lateral and longitudinal positions chosen can always vary for a straight line scar but are dependent on the radius of the curved surface that the curved or arc line scar subtends.

Couch Vertical positions correspond to the positive and negative z-plane, i.e. superior-inferior. Couch lateral positions correspond to positive and negative x-plane, i.e. cross-section or right-left. Couch longitudinal positions correspond to the positive and negative y-plane, i.e. anterior-posterior. The couch positions for each coordinate point on a scar were generated by using the following equations.

$$Vrt_i = Vrt_0 + Y_i \qquad \text{Eqn. 3}$$

i=1to N. N is the total number of target points or index. Where Vrt_i, Vrt_0 and Y_i are couch vertical position at index i, initial vertical position and scar vertical coordinate value, respectively.

$$Lat_i = Lat_0 + X_i \qquad \text{Eqn. 4}$$

i=1to N. Where Lat_i, Lat_0 and X_i are couch lateral position at index i, initial couch lateral position and scar lateral coordinate value respectively.

$Lng_i=Lng_0+Z_i$. Eqn. 5

i=1to N. Where Lng_i, Lng_0 and Z_i are couch longitudinal position at index i, initial couch longitudinal position and scar vertical coordinate value respectively.

Collimator Angle

Collimator angle must be set at zero and kept constant throughout the treatment delivery if cutout used is a circular cutout. However in this study a $3x3cm^2$ cutout was used, hence the collimator angle changes/rotates during treatment.

At target point index *i*, the collimator is rotated so that it always points to the next point. In the beams-eye-view (BEV), the initial target point (*i*) has coordinates (0, 0, 0). The next target point (*i*+1) has coordinate points (dx, dy, dz). Where $dx=x_{i+1}-x_i$, $dy=y_{i+1}-y_i$, $dz=z_{i+1}-z_i$. These coordinates are in the original CT scar coordinates used in deriving the other parameters discussed above.

The coordinates for the initial target point (*i*) and the next target point (i+1), which are in the CT coordinate system needs to be transformed to the BEV coordinate system. The BEV coordinate system has a gantry angle rotation of θ_i, where *i*=1toN.

In the BEV coordinate system, initial target point (*i*) has coordinates (0, 0, 0) and the next target point (*i*+1) has coordinates (dx', dy', dz'), where $dx'=dx(\cos\theta_i)- dy(\sin\theta_i)$, $dy'= dy(\cos\theta_i)+dx(\sin\theta_i)$, $dz'=dz$.

From the above derivations it follows that the collimator angle, φ_i satisfies the equation, $\tan \varphi_i = dz'/dx'$.

MU

The MU for the scar targets is computed from the equation below.

$$MU_0 = \frac{Prescription\ Dose\ (cGy)}{CF_{SSD} \times OF_{Cone\_Cutout} \times IDL \times ISF} \quad \text{Eqn. 6}$$

Where MU_o is the MU for the first point or single field along the scar to be irradiated, CF_{SSD} is the calibration factor at SSD, OF_{cone_cutout} is the cone/cutout factor, IDL is the prescription isodose line and ISF is the inverse square.

To compute the total MU needed to irradiate an entire scar, the following equation is used:

$$MU_T = (L/W) * MU_o \quad \text{Eqn. 7}$$

Where MU_T is the total MU for a particular scar, L is the total length of the scar to be treated, MU_o is MU computed for first point or single field along the scar length, W is the width of the single field, i.e. width of cutout.

MU calculation is done with static beamlets. These static beamlets become a dynamic beam during plan delivery. These static beamlets can be represented as control points (CP), where each control point corresponds to the amount of MU to be delivered to that point.

Table 1: MU calculation for every control point (CP). The total number of target points (N) corresponds to the number of coordinates given in the CT scar data.

CP	Gantry Angle	MU @ CP	MU
1	θ_1	$(MU_0/w)*L_1$	MU_1
2	θ_2	$MU_1+(MU_0/w)*L_2$	MU_2
3	θ_3	$MU_2+(MU_0/w)*L_3$	MU_3
.	.	.	.
.	.	.	.
.	.	.	.
.	.	.	.
N	θ_N	$MU_{N-1}+(MU_0/w)*L_N$	MU_N

2.1 Dynamic electron arc radiotherapy algorithm for irradiating a straight line scar and curved or arc line scar.

The demonstration of the feasibility and accuracy of using the DEAR technique to irradiate scars was done by using a straight line scar and curved or arc line scar. In this section the process of developing a DEAR algorithm to create a treatment plan for both the straight line scar and arc scar will be outlined.

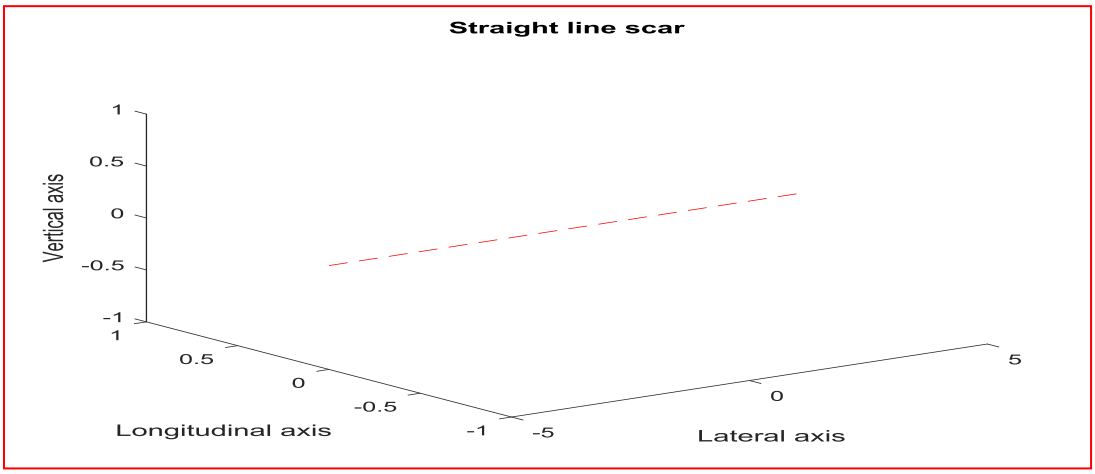

Figure 5: A 3D representation of the straight line scar. Plot is done using scar coordinates extracted from a CT image of the scar.

Gantry angle

The Gantry angle for the straight line scar is 180°. The angle is constant throughout the delivery.

Generating couch positions

The couch positions for each coordinate point on line scar 1 are generated by using the following equations (1), (2), (3), (4) and (5).

- $Vrt_i = Vrt_0 + Y_i$, i=1:N

N is the total number of target points or index and in this particular case N=11.

Where Vrt_i, Vrt_0 and y_i are couch vertical position at index i, initial vertical position and scar vertical coordinate value, respectively.

Y_i=0cm

Vrt_0=100cm

Vrt_i=100cm, for all indexes, i.e. i=1:11. Couch Vertical positions are all 100cm

- $Lat_i = Lat_0 + X_i$, i=1:N

Where Lat_i, Lat_0 and X_i are couch lateral position at index i, initial couch lateral position and scar lateral coordinate value respectively.

X_i= -5cm

Lat_0=94cm

Lat_i=95cm: 105cm, for all indexes i.e. i=1: 11. Couch lateral positions range from 95cm to 105cm.

- $Lng_i = Lng_0 + Z_i$, i=1:N

Where Lng_i, Lng_0 and Z_i are couch longitudinal position at index i, initial couch longitudinal position and scar vertical coordinate value respectively.

Lng_0=115cm

Z_i=0cm

Lng_i =115cm, for all indexes i.e. i=1:11 i.e. Couch longitudinal positions are all 115cm

MU calculations

Cone=6X6cm^2

Cutout=3X3cm^2

Prescription dose= 200cGy to dmax.

CF_{SSD}=1.0cGy/MU for SSD=100cm

OF_{cone_cutout} =0.867, from Electron cone and cutout factor table data obtained from TrueBeam Linac at DUMC.

IDL=1.0, dose prescription is to dmax or 100% isodose line.

ISF = 1.0

MU_o =230.68MU from calculation using Eqn. 6

L= 10cm, length of scar to be treated

W=3cm, width of field i.e. width of cutout

MU_T =768.93MU, total MU needed to treat entire straight line scar.

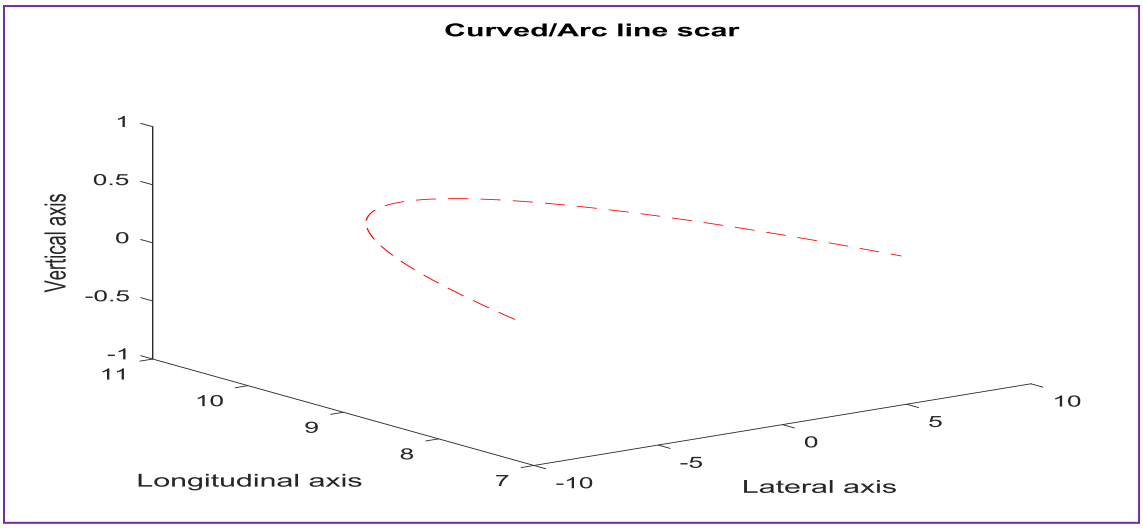

Figure 6: A 3D representation of the curved/arc line scar. Plot is done using scar coordinates extracted from CT image of the scar.

Gantry angles

Theta, θ values ranging from -45° to 45° are given and from these θ values the corresponding gantry angles are generated using the equation below,

Gantry angle$_i$=180°- θ_i. i=1:91. The corresponding gantry angles ranges from 225° to 135° in 1° increments.

Generating couch positions

The couch positions for each coordinate point on curved/arc scar were generated by using the following equations.

- $Vrt_i=Vrt_0+Y_i$, i=1:N.

N is the total number of target points or index and in this particular case N=91

Where Vrt_i, Vrt_0 and Y_i are couch vertical position at index i, initial vertical position and scar vertical coordinate value respectively.

Y_i=7.778cm

Vrt_0=118.15cm

Vrt_i=125.928cm: 125.928cm, for all indexes i.e. i=1:91 i.e. Couch Vertical positions range from125.928cm to 125.928cm reaching a maximum value of 129.150cm at 180^o gantry angle.

- $Lat_i=Lat_0+X_i$, i=1:N

Where Lat_i, Lat_0 and X_i are couch lateral position at index i, initial couch lateral position and scar lateral coordinate value respectively.

X_i= -7.778cm

Lat_0=100cm

Lat_i=107.778cm: 92.222cm, for all indexes i.e. i=1:91 i.e. Couch lateral positions range from 107.778cm to 92.222cm.

- $Lng_i=Lng_0+Z_i$, i=1:N

Where Lng_i, Lng_0 and Z_i are couch longitudinal position at index i, initial couch longitudinal position and scar vertical coordinate value respectively.

Lng_0=90.420cm

Z_i=0cm

Lng_i=90.420cm, for all indexes i.e. i=1:91 i.e. Couch longitudinal positions are all 90.420cm.

MU calculations

Cone=6X6cm^2

Cutout=3X3cm^2

Prescription dose= 400cGy to dmax (*Measurement was not done at dmax)

CF_{SSD}=1.0cGy/MU for SSD=100cm

OF_{cone_cutout} =0.867, from Electron cone and cutout factor table data obtained from TrueBeam Linac at DUMC

IDL=1.0, dose prescription is to dmax or 100% isodose line.

ISF = 1.0

MU_o = 461.59MU from calculation.

L= 17.28cm, length of scar to be treated.

W=3cm, width of field, i.e. width of cutout.

MU_T = 2657.43 MU, total MU needed to treat entire curved/arc line scar.

2.1.1 Eclipse system plan design and Monte Carlo simulation

Plans were designed for the straight line scar and the curved/arc line scar in the Eclipse Treatment Planning System (Varian Medical Systems, Inc., Palo Alto, CA). A square phantom was created and used as a flat surface. Twenty (20) fields were arranged according to the x, y and z coordinates of the straight line scar CT image as shown in figure 8. The beam fields irradiated a 10 cm straight line similar to the length of the straight line scar. The gantry angle and couch rotation were kept constant. The couch moved laterally from 95 cm to 105 cm but the couch did not move vertically and longitudinally.

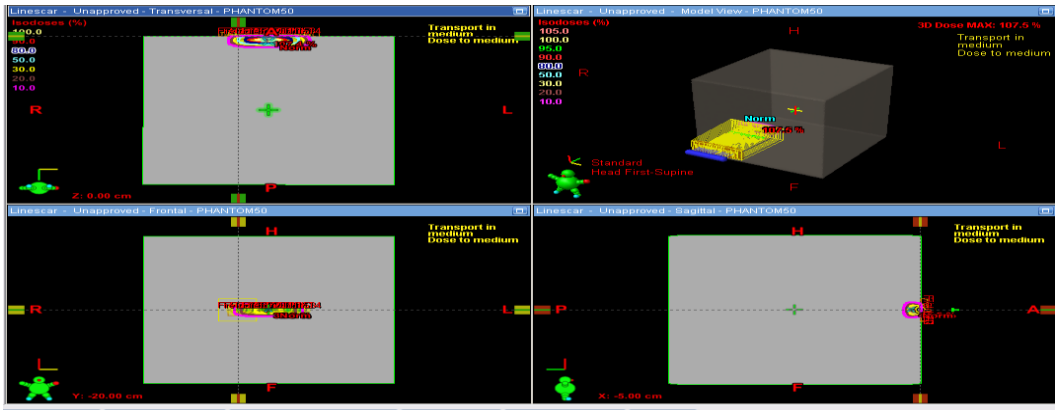

Figure 7: Screen capture showing straight line scar plan design in Eclipse TPS.

A cylindrical phantom was created and used as a curved surface. Nineteen (19) fields were arranged according to the x, y and z coordinates of the curved/arc scar CT image as can be seen in figure 8. The beam fields irradiated a 17.28cm curved line along

the surface of the cylinder. The gantry angle move through an angle of 90^0 anticlockwise whiles the couch movement is from 107.778 cm to 92.222 cm laterally and a total of 14 cm vertically. Couch did not move longitudinally.

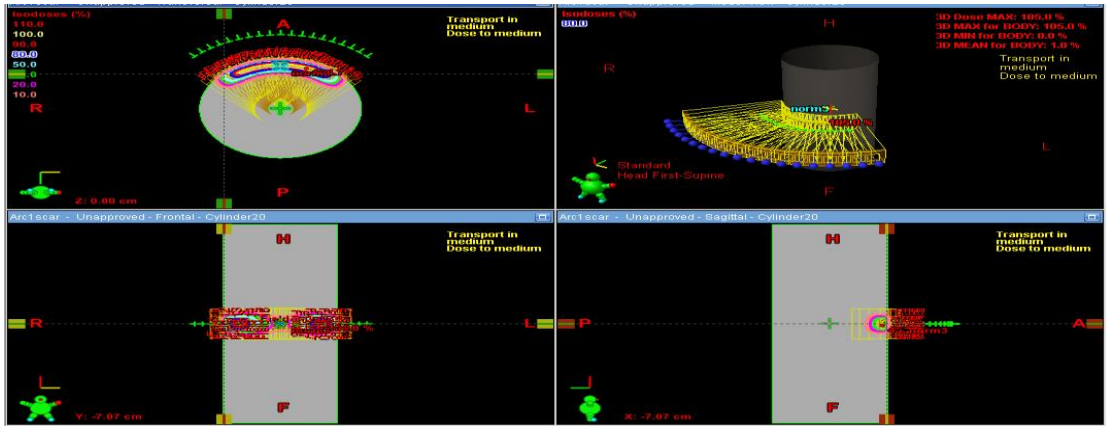

Figure 8: Screen capture showing curved/arc line scar plan design in Eclipse TPS.

The dose profile data for the computed dose was extracted for comparative analysis. The virtual Linac in the Eclipse TPS was used to design plans for the two scar types: straight line and curved/arc scar. Depth doses and dose profiles were generated by Monte Carlo simulations. The comparisons between the Monte Carlo simulated, TPS calculated and gafchromic film measured dose profiles were analyzed.

2.1.2 Plan Delivery

The designed plans were created using parameters like the gantry rotation, couch movement (vertical, horizontal and lateral) and Monitor Units (MU) were loaded into a Spreadsheet based Automatic Generator (SAGE) software (Varian Medical Systems, Inc.,

Palo Alto, CA). The eXtensible Markup Language (XML) file generated by the SAGE software which can be seen in figure 9 was run on a TrueBeam Linac in research mode. Delivery was done on i) a solid water phantom for a scar on a flat surface and ii) a cylindrical phantom of radius 11cm for a scar on a curved surface. The square flat surface of the solid water phantom was used to simulate the irradiation of a straight line target or scar on a flat surface. The curved surface of the cylindrical phantom was used to simulate the irradiation of a curved or arc line target on a curved surface. Energy used was 6 MeV, 6x6 cm^2 applicator fitted with a 3x3 cm^2 cutout. A 95 cm standard applicator is fitted to the Linac head and the SSD used was 100 cm. Gafchromic film was used to measure the planar dose. The film was placed at a depth of 1.5 cm in the solid water phantom for the straight line plan design delivery. The surface of the cylindrical phantom was covered with the gafchromic film as shown in figure 11, for the arc line plan delivery. The trajectory log files produced were analyzed for deliverability and film dose profiles compared to dose profiles from plans designed in Eclipse TPS and also from the Virtual Linac using the Monte Carlo method.

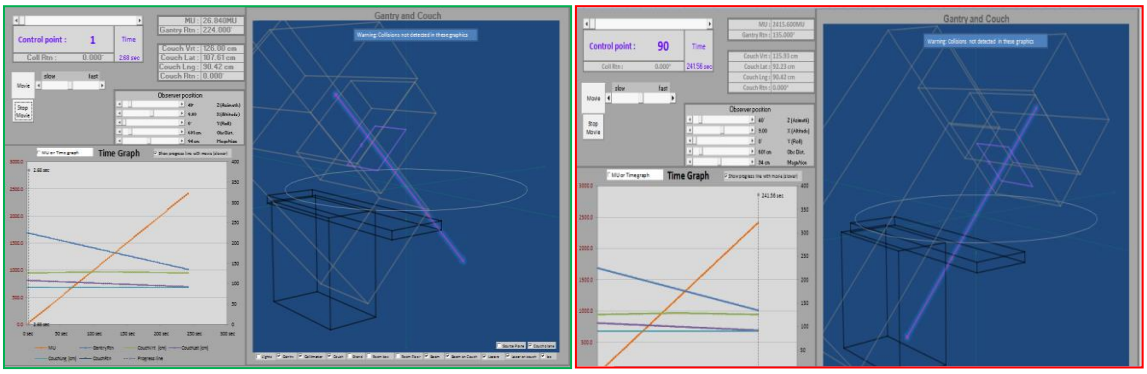

Figure 9: Varian SAGE software simulation of treatment plan for the DEAR technique. Initial mechanical axes positions (green box). Final mechanical axes positions (red box)

Figure 10: Delivery of DEAR technique on a Varian TrueBeam Linac in research mode. The machine is delivering a plan designed in XML format loaded onto the machine control console computer.

Figure 11: Delivery of straight line scar plan design. Film is placed at 1.5 cm depth in solid water phantom (violet box) and curved/arc line scar design. Film is attached to the surface of cylindrical phantom (red box).

2.2 Analysis of delivered plans

Mechanical accuracy: The delivered straight line scar and curve/arc scar plans were analyzed in terms of mechanical and dosimetric accuracy. Mechanical accuracy was verified with regards to the accuracy of the gantry rotation, couch movements (lateral, vertical and longitudinal) and MU. The trajectory log file is a file generated by the TrueBeam Linac when it delivers a treatment plan in research mode. The Linac computer system records an actual and expected trajectory every 20 ms during delivery. The expected trajectory is recorded taking into account the machine limitations and it is taken from the intended trajectory which is specified in the XML file. The RMSE equation is

used to calculate the degree of agreement between the expected and actual axes values recorded in the trajectory log files.

$$RMSE = \sqrt{\frac{1}{n}\sum_{k=1}^{n}(y_k - \hat{y}_k)\text{^}2}$$

Eqn. 8

Where y_k the actual trajectory axis value and $\hat{y}_k$ is the expected trajectory axis value.

Dosimetry analysis: The gafchromic film used for measuring the dose was read with a film scanner. The dose from the scanned film as shown in figure 12 was read with a Matlab code. In-plane and cross-plane dose profiles were plotted using data from scanned film dose.

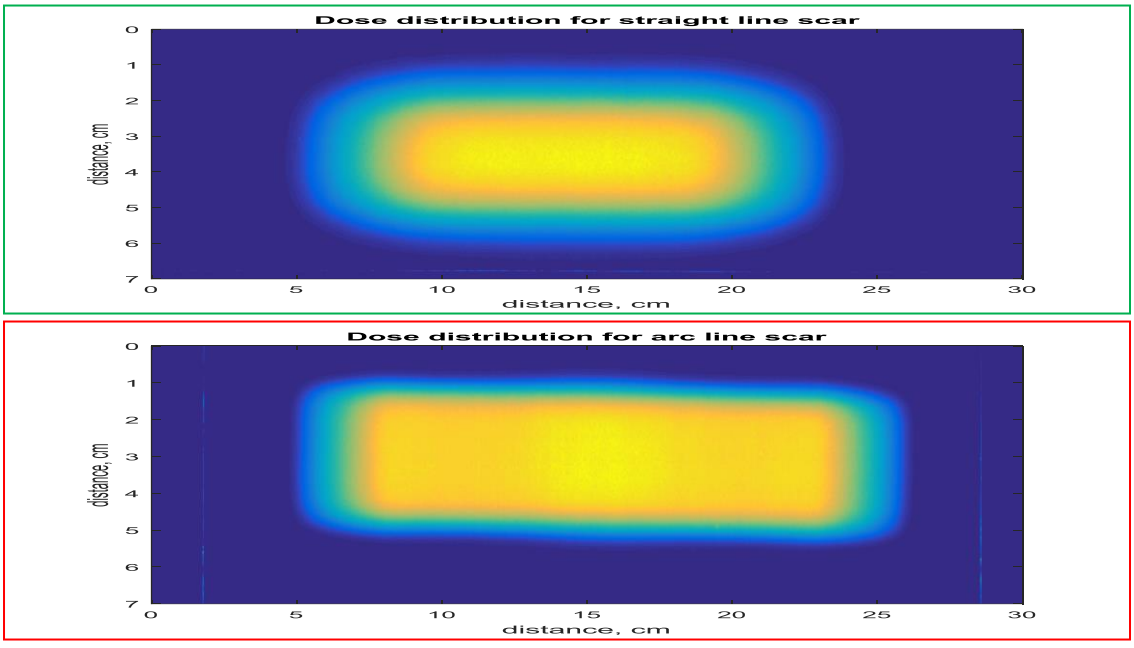

Figure 12: Scanned film dose distribution for straight line and arc line scars.

3. Results

The trajectory log and XML files were used to analyze the mechanical accuracy or deliverability of the plans designed to irradiate the straight line scar and arc line scar. The mechanical axes values were categorized into expected and actual axes values derived from the trajectory log files and intended axes values derived from the XML files. Figure 13 and figure 14 show trajectory log analysis plots of mechanical axes values and MU values for arc line scar and straight line scar. It is important to note the high level of correlation between the three (3) plotted lines i.e. expected, actual and intended. The intended axes values, which are the gantry angle, couch lateral, couch longitudinal, couch vertical and MU values, were assigned to each control point in the treatment planning XML file. The main objective of this analysis is to ascertain the degree of agreement between the intended axes values extracted from the planning file to irradiate the scar and the actual axes values extracted from the log files after the plan has been delivered.

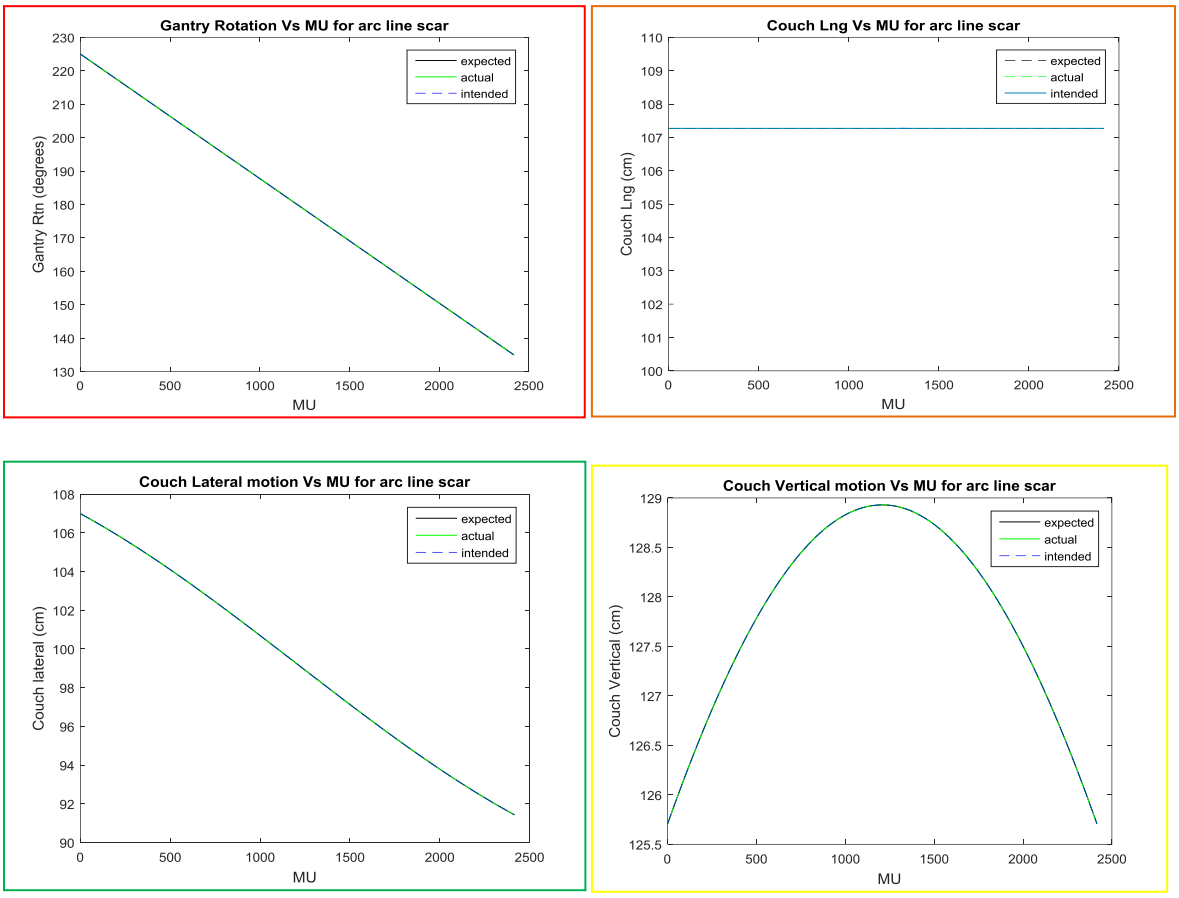

Figure 13: Plots of Gantry rotation and couch motion axes against MU for arc line scar.

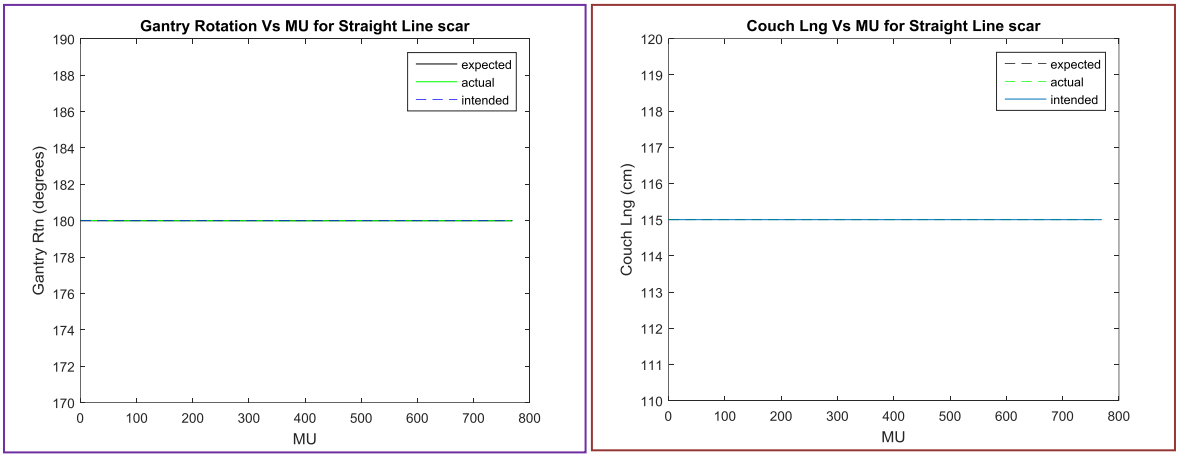

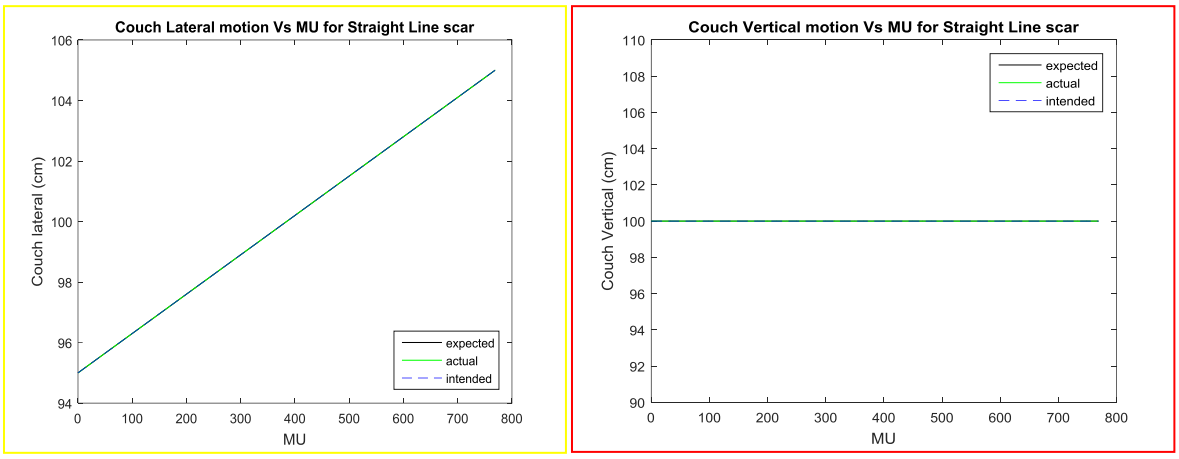

Figure 14: Plots of Gantry rotation and couch motion axes against MU for Straight line scar.

The mechanical accuracy is verified using the root mean square error (RMSE) to calculate the degree of agreement between the intended axes values from the XML file and actual axes values from the trajectory log files as shown in table 2. The root mean square error (RMSE) for the line scar is approximately 0.0035^0 Gantry angle and it is 0.0349 for arc scar, this is due to the fact that in the straight line delivery the gantry is static so it has a higher degree of agreement than in the arc delivery. RMSE values for the straight line scar has an overall high degree of agreement compared to the arc scar because the arc scar delivery has more mechanical axes motion during delivery. This high degree of agreement show that the plans designed to irradiate surgical scars using DEAR can be delivered with high accuracy by a TrueBeam Linac (Varian Medical Systems, Inc., Palo Alto, CA) in research mode.

Table 2: RMSE values showing degree of agreement between actual and intended mechanical axe values extracted from trajectory log files XML plan files.

Scar type	RMSE for Gantry Rotation(^{0})	RMSE for Couch lateral motion (cm)	RMSE for Couch Vertical motion(cm)	RMSE for Couch Longitudinal motion (cm)
Straight line Scar	0.0035	8.31×10^{-4}	6.40×10^{-4}	7.60×10^{-4}
Curved/arc Scar	0.0349	6.16×10^{-4}	5.99×10^{-4}	2.72×10^{-5}

The dose profile analysis show that the designed plans for the straight line and arc line scars are delivered with good dosimetric accuracy as can be seen in Figure 15. The Eclipse Treatment Planning System (TPS) is not designed for planning dynamic electron therapy techniques such as DEAR which involves the motion of multiple mechanical axes. Thus a series of small overlaps of fields are used to simulate a dynamic delivery. The field overlaps are not small enough to produce dose distributions similar to a virtual Linac dynamic beam simulation. In addition to non-uniform dose it is also manually tasking to improve dose distributions by using a lot of beam fields. In Eclipse TPS the electron Monte Carlo (eMC) algorithm is used for dose calculations.

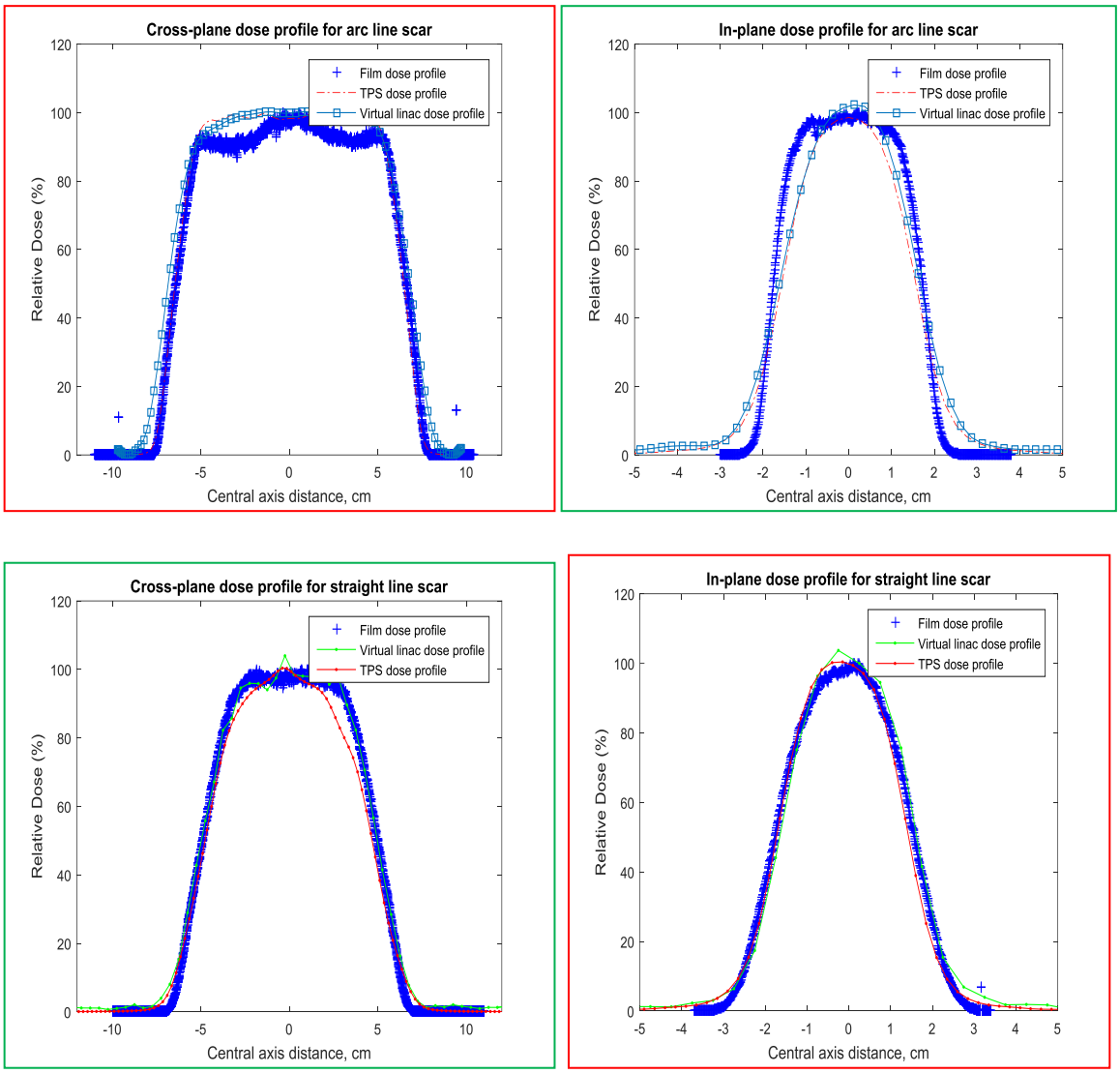

Figure 15: Dose profiles showing the degree of agreement between measured film dose and calculated dose (Eclipse TPS eMC and Virtual Linac).

The dose profiles were normalized such that a relative comparison can be done between the Eclipse TPS eMC calculation, Virtual Linac Monte Carlo calculation and film dose measurement. All the profiles were normalized to the value on the central axis.

4. Discussion

This research was done to demonstrate the feasibility of using dynamic electron arc radiotherapy technique to irradiate surgical scars on flat and curved surfaces. During delivery, a 3x3 cm cut-out was used, but in more conventional techniques a 3x10 cm cut-out can be used hence there will be no need for the couch to move during delivery, if the scar is a straight line scar on a flat surface but not all scars are straight lines and also not all scars occur on flat surfaces. A 3x10 cm cutout can be used but it has drawbacks if the surface is not flat, such as non-uniform dose distribution.

Also a cutout that covers the entire scar can be used if the scar size is small e.g. less than 10 cm; if the scar is big e.g. 40 cm long and the maximum cone size is 20x20cm. The problems stated above will occur. It must be noted that scar shapes are not always straight lines, nor do they always occur on a flat surfaces. Different patients have different scars, requiring a cutout for every patient which is not ideal. The DEAR technique allows one small cutout to be used to treat different scars of any length and on any surface. The small aperture utilized produced uniform dose distributions for both large and small targets. Further studies should be done on diagonal and spiral scars, and plans designed for the treatment of such scars should be delivered and analyzed dosimetrically. Also, research work should be done on developing QA procedures for this technique.

5. Conclusion

The dynamic electron arc radiotherapy as a novel treatment modality was used to plan and deliver radiation to superficial scars. The results obtained showed that the DEAR technique can be used to treat various line targets (scars) i.e. straight or arc scar to a high degree of accuracy. This treatment modality can help reinvigorate electron therapy and make it a clinically viable treatment option.

Appendix A

Diagonal line and Spiral scar plan designs

Control Point #	Time [sec]	MU	GantrgRtn	Couch Vrt (cm)	Couc hLat (cm)	Couc hLng (cm)
0	0.0000	0.000	180.0	100	96.464	111.464
1	2.6840	76.890	180.0	100.000	97.172	112.172
2	5.3760	153.780	180.0	100.000	97.879	112.879
3	8.0670	230.670	180.0	100.000	98.586	113.586
4	10.7560	307.560	180.0	100.000	99.293	114.293
5	13.4450	384.450	180.0	100.000	100.000	115.000
6	16.1340	461.340	180.0	100.000	100.707	115.707
7	18.8230	538.230	180.0	100.000	101.414	116.414
8	21.5120	615.120	180.0	100.000	102.121	117.121
9	24.2010	692.010	180.0	100.000	102.828	117.828
10	26.8900	768.900	180.0	100.000	103.536	118.536

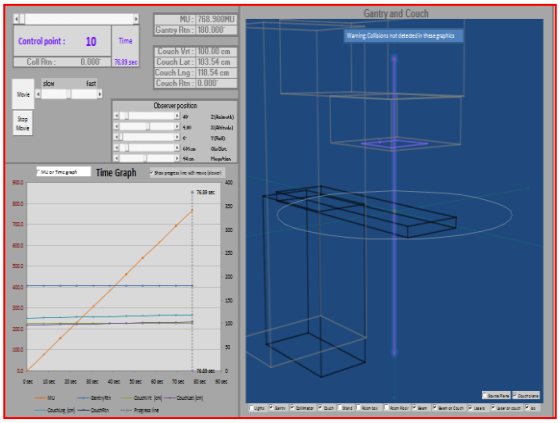

Figure 16: Plan design for diagonal scar (blue box) SAGE simulation for diagonal scar.

Control Point #	Time (sec)	MU	Gantry Rtn	Couch Vrt (cm)	Couch Lat (cm)	Couch Lng (cm)
0	0.0000	0.000	225.0	115	107	125.00
1	2.6840	26.840	224.0	115.065	106.84	125.11
2	5.3680	53.680	223.0	115.130	106.69	125.22
3	8.0520	80.520	222.0	115.195	106.53	125.33
4	10.7360	107.360	221.0	115.260	106.38	125.44
5	13.4200	134.200	220.0	115.325	106.22	125.56
6	16.1040	161.040	219.0	115.390	106.06	125.67
7	18.7880	187.880	218.0	115.455	105.91	125.78
8	21.4720	214.720	217.0	115.520	105.75	125.89
9	24.1560	241.560	216.0	115.585	105.6	126.00
10	26.8400	268.400	215.0	115.650	105.44	126.11
11	29.5240	295.240	214.0	115.715	105.28	126.22
12	32.2080	322.080	213.0	115.780	105.13	126.33
13	34.8920	348.920	212.0	115.845	104.97	126.44
14	37.5760	375.760	211.0	115.910	104.82	126.55
15	40.2600	402.600	210.0	115.975	104.66	126.67
16	42.9440	429.440	209.0	116.040	104.5	126.78
17	45.6280	456.280	208.0	116.105	104.35	126.89
18	48.3120	483.120	207.0	116.170	104.19	127.00
19	50.9960	509.960	206.0	116.235	104.04	127.11
20	53.6800	536.800	205.0	116.300	103.88	127.22
21	56.3640	563.640	204.0	116.365	103.72	127.33
22	59.0480	590.480	203.0	116.430	103.57	127.44
23	61.7320	617.320	202.0	116.495	103.41	127.55
24	64.4160	644.160	201.0	116.560	103.26	127.66
25	67.1000	671.000	200.0	116.625	103.1	127.78
26	69.7840	697.840	199.0	116.690	102.94	127.89
27	72.4680	724.680	198.0	116.755	102.79	128.00
28	75.1520	751.520	197.0	116.820	102.63	128.11
29	77.8360	778.360	196.0	116.885	102.48	128.22
30	80.5200	805.200	195.0	116.950	102.32	128.33
31	83.2040	832.040	194.0	117.015	102.16	128.44
32	85.8880	858.880	193.0	117.080	102.01	128.55
33	88.5720	885.720	192.0	117.145	101.85	128.66
34	91.2560	912.560	191.0	117.210	101.69	128.77
35	93.9400	939.400	190.0	117.275	101.54	128.88
36	96.6240	966.240	189.0	117.340	101.38	128.99
37	99.3080	993.080	188.0	117.405	101.23	129.10
38	101.9920	1019.920	187.0	117.470	101.07	129.21
39	104.6760	1046.760	186.0	117.535	100.91	129.32
40	107.3600	1073.600	185.0	117.600	100.76	129.43
41	110.0440	1100.440	184.0	117.665	100.6	129.54
42	112.7280	1127.280	183.0	117.730	100.45	129.65
43	115.4120	1154.120	182.0	117.795	100.29	129.76
44	118.0960	1180.960	181.0	117.860	100.13	129.87
45	120.7800	1207.800	180.0	117.925	99.98	129.98
46	123.4640	1234.640	179.0	117.990	99.82	130.09
47	126.1480	1261.480	178.0	118.055	99.67	130.20
48	128.8320	1288.320	177.0	118.120	99.51	130.31
49	131.5160	1315.160	176.0	118.185	99.35	130.42
50	134.2000	1342.000	175.0	118.250	99.2	130.53
51	136.8840	1368.840	174.0	118.315	99.04	130.64
52	139.5680	1395.680	173.0	118.380	98.89	130.75
53	142.2520	1422.520	172.0	118.445	98.73	130.86
54	144.9360	1449.360	171.0	118.510	98.57	130.97
55	147.6200	1476.200	170.0	117.275	98.42	131.11
56	150.3040	1503.040	169.0	117.210	98.264	131.22
57	152.9880	1529.880	168.0	117.145	98.108	131.33
58	155.6720	1556.720	167.0	117.080	97.952	131.44
59	158.3560	1583.560	166.0	117.015	97.796	131.55
60	161.0400	1610.400	165.0	116.950	97.64	131.66
61	163.7240	1637.240	164.0	116.885	97.484	131.77
62	########	1664.080	163.0	116.820	97.328	131.88
63	########	1690.920	162.0	116.755	97.172	131.99
64	171.7760	1717.760	161.0	116.690	97.016	132.10
65	174.4600	1744.600	160.0	116.625	96.86	132.22
66	177.1440	1771.440	159.0	116.560	96.704	132.33
67	179.8280	1798.280	158.0	116.495	96.548	132.44
68	182.5120	1825.120	157.0	116.430	96.392	132.55
69	185.1960	1851.960	156.0	116.365	96.236	132.66
70	187.8800	1878.800	155.0	116.300	96.08	132.77
71	190.5640	1905.640	154.0	116.235	95.924	132.88
72	########	1932.480	153.0	116.170	95.768	132.99
73	195.9320	1959.320	152.0	116.105	95.612	133.10
74	198.6160	1986.160	151.0	116.040	95.456	133.21
75	########	2013.000	150.0	115.975	95.3	133.33
76	########	2039.840	149.0	115.910	95.144	133.44
77	########	2066.680	148.0	115.845	94.988	133.55
78	########	2093.520	147.0	115.780	94.832	133.66
79	########	2120.360	146.0	115.715	94.676	133.77
80	214.7200	2147.200	145.0	115.650	94.52	133.88
81	217.4040	2174.040	144.0	115.585	94.364	133.99
82	########	2200.880	143.0	115.520	94.208	134.10
83	########	2227.720	142.0	115.455	94.052	134.21
84	########	2254.560	141.0	115.390	93.896	134.32
85	########	2281.400	140.0	115.325	93.74	134.44
86	########	2308.240	139.0	115.260	93.584	134.55
87	########	2335.080	138.0	115.195	93.428	134.66
88	########	2361.920	137.0	115.130	93.272	134.77
89	########	2388.760	136.0	115.065	93.116	134.88
90	241.5600	2415.600	135.0	115.000	92.96	134.99

Figure 17: Plan design for spiral scar.

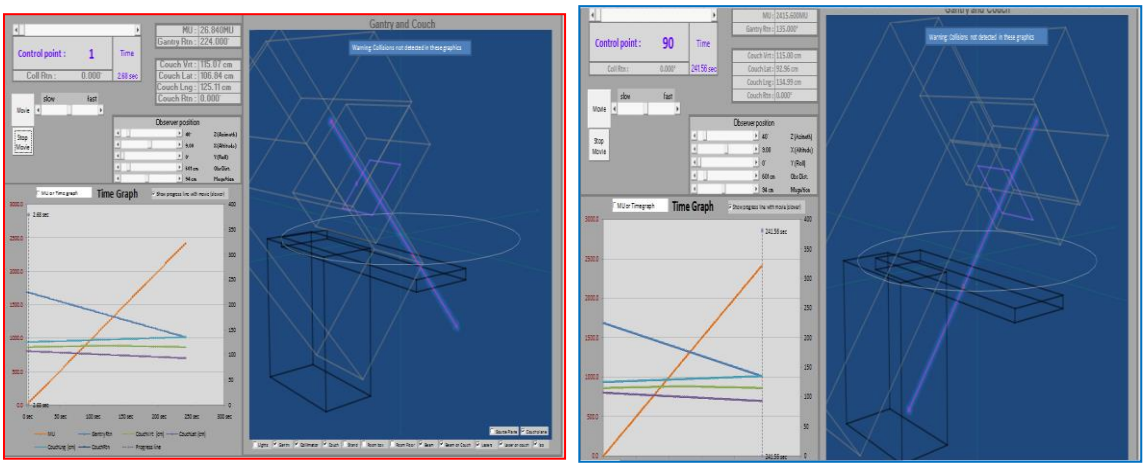

Figure 18: SAGE simulation of spiral scar.

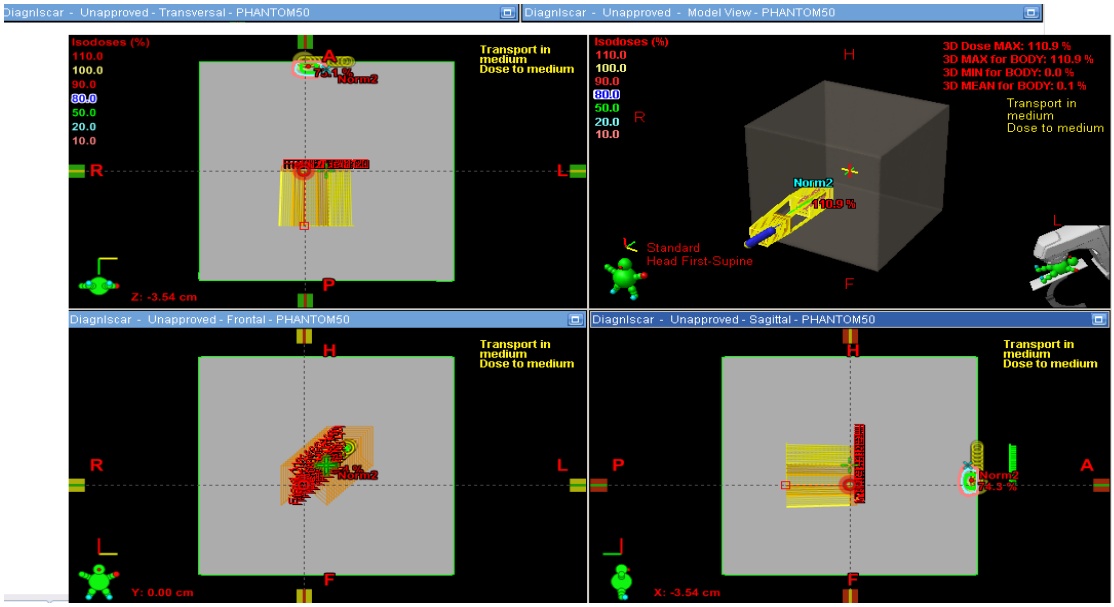

Figure 19: Eclipse TPS plan design for diagonal scar on surface of cubic phantom.

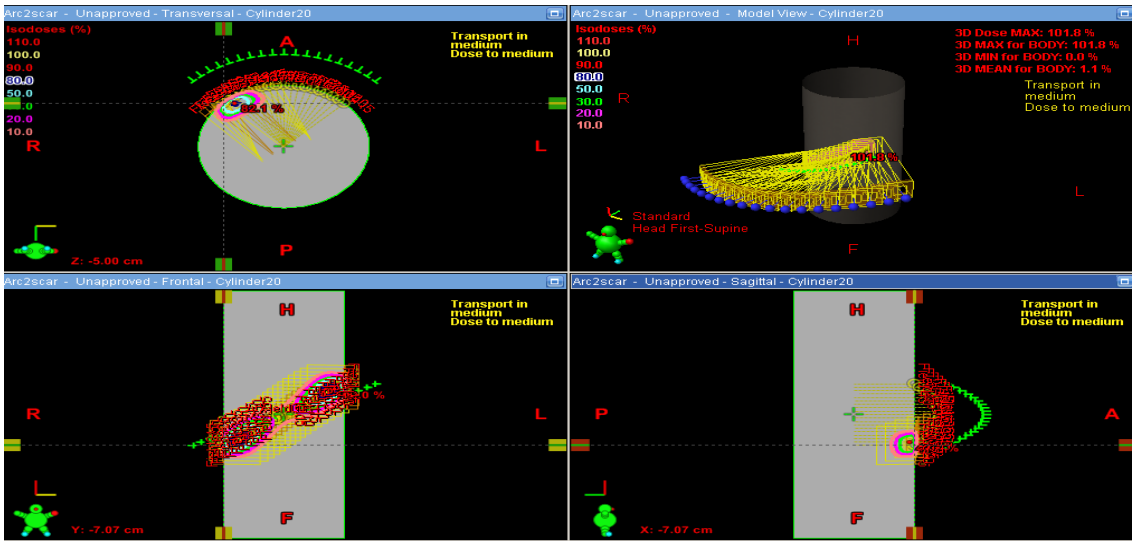

Figure 20: Eclipse TPS plan design for spiral scar on surface of cylindrical phantom.

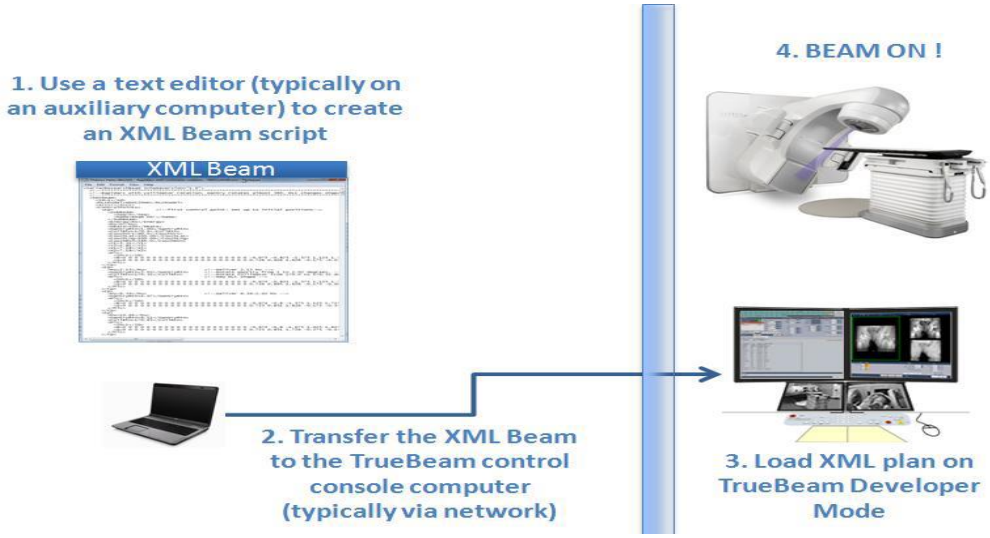

Figure 21: The process of DEAR delivery on TrueBeam Linac. (TrueBeam™ Developer Mode. Version 2.0 User's Manual, Varian Medical Systems)

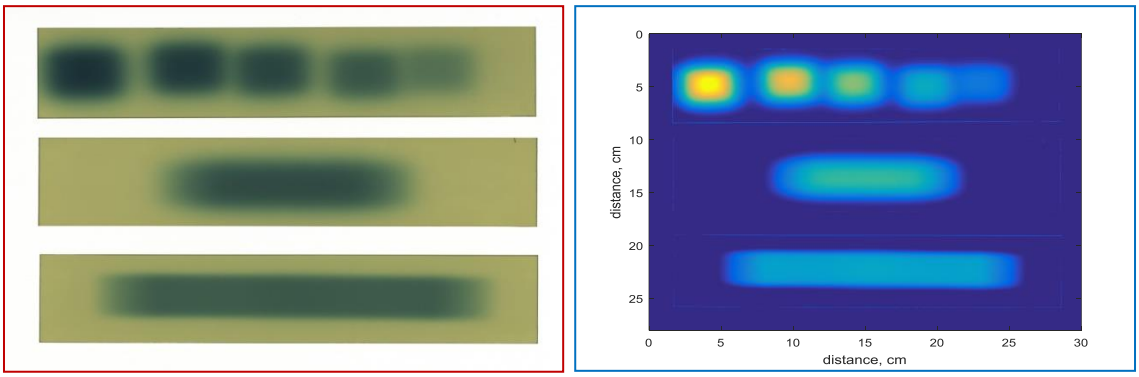

Figure 22: Film showing delivered dose for static delivery, straight line scar and arc scar deliveries (red box). Film scanned dose (blue box).

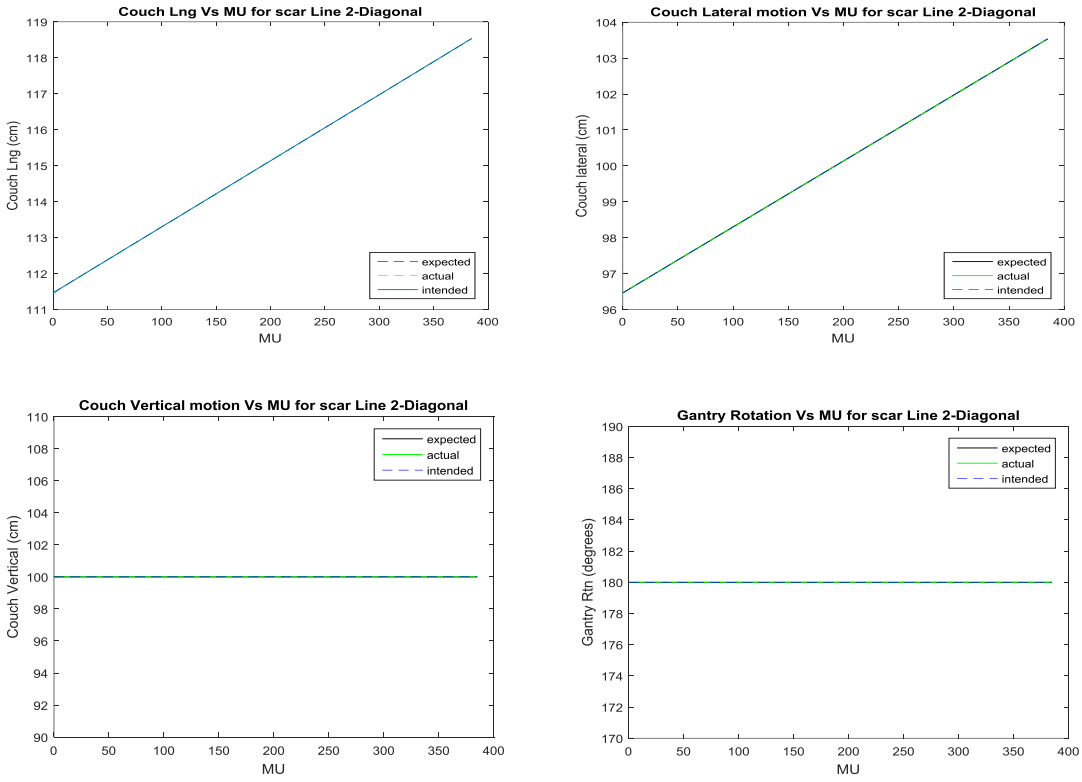

Figure 23: Plots of expected, actual and intended mechanical axes values from XML and trajectory log files for diagonal scar.

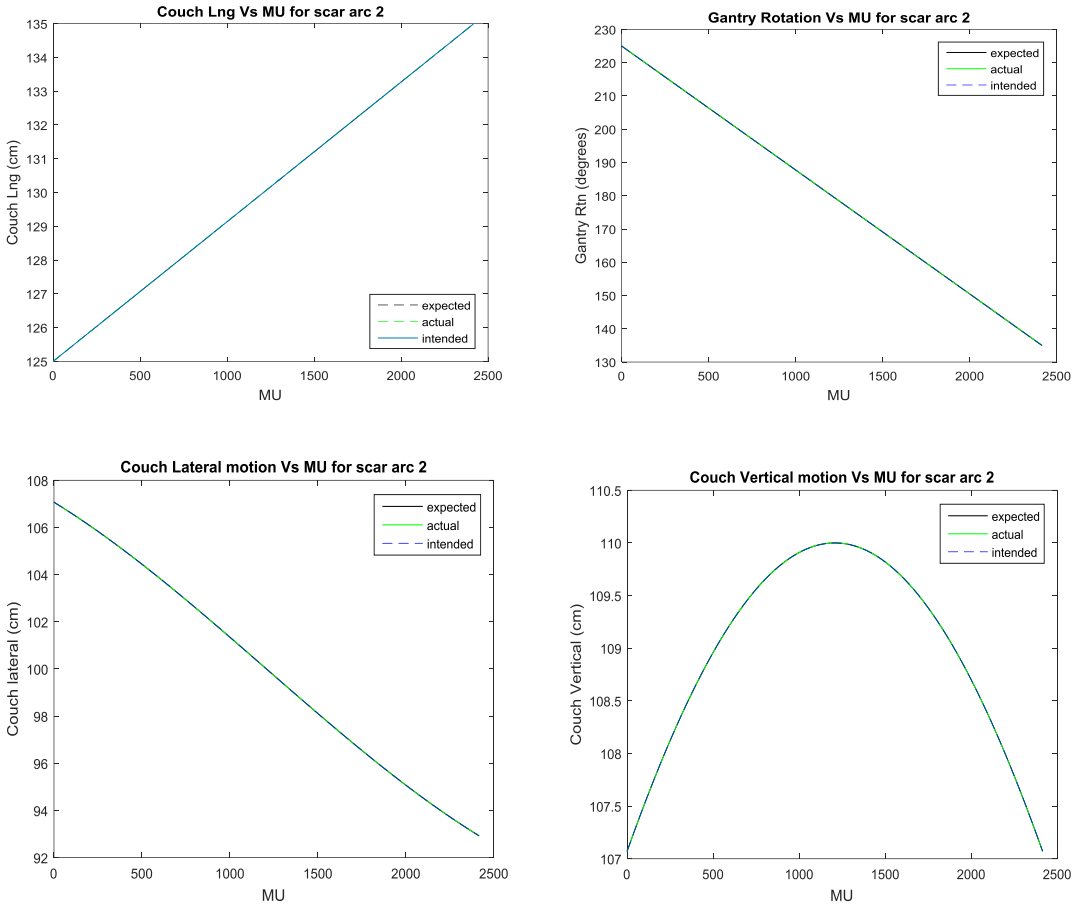

Figure 24: Plots of expected, actual and intended mechanical axes values from XML and trajectory log files for spiral scar.

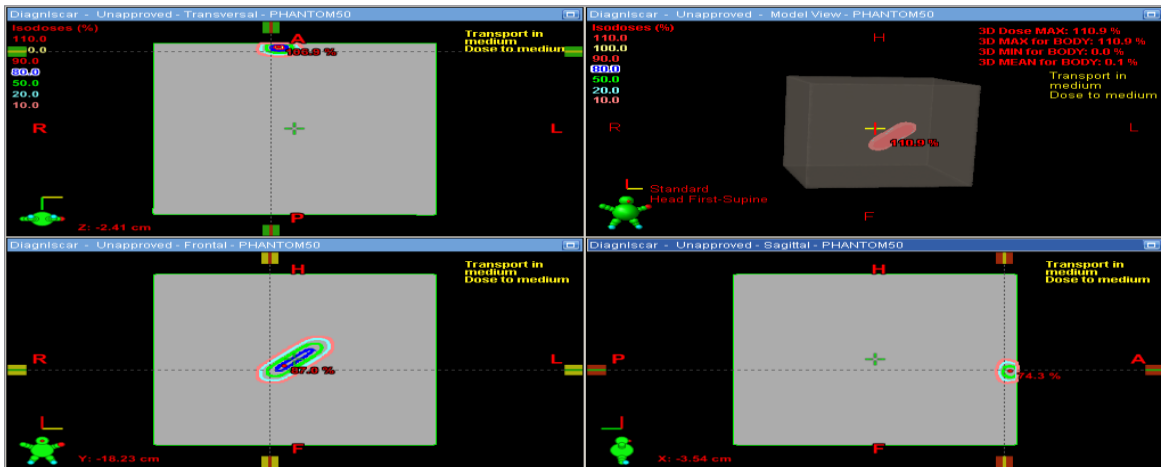

Figure 25: Dose distribution of diagonal scar obtained from dose calculation using Eclipse TPS eMC algorithm.

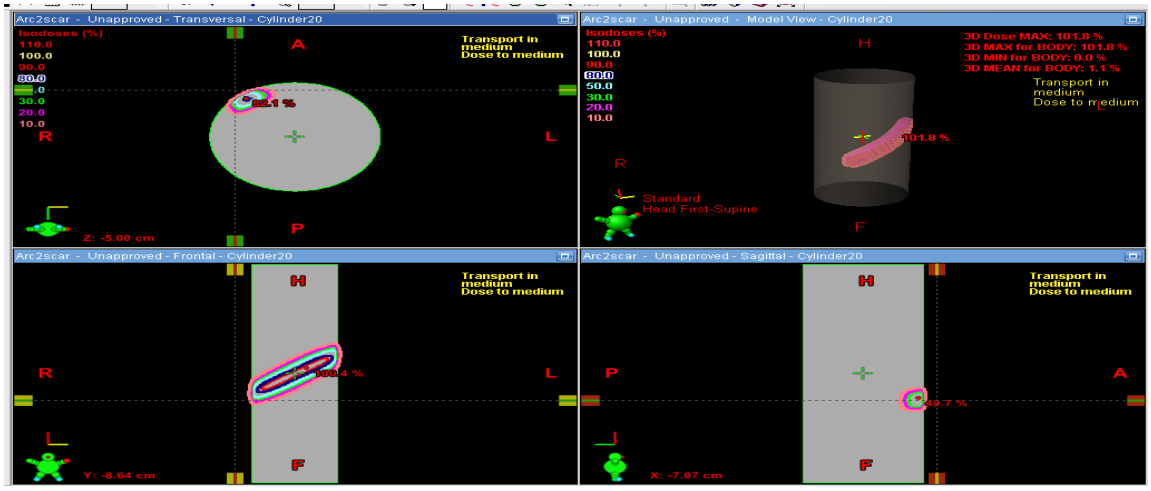

Figure 26: Dose distribution of spiral scar obtained from dose calculation using Eclipse TPS eMC algorithm.

Appendix B

MATLAB codes used for deliverability analysis and dosimetric analysis.

Generation of Trajectory plots from XML and log files.

Calculation of RMSE.

```
%% Reading mechanical axes values from SAGE software.
% Axes values inputed into SAGE software to generate XML file.
% Generating plots for intended, expected and actual mechanical axes
% trajectories.
% Input data from plan designs for all scar types given i.e. straight
line,
% arc, diagonal and spiral.
[header, sub, data] = TrajLogReader_v2();
filename = 'SAGE-Line1';
sheet = 7;
x1Range = 'B40:H50';
xml_outL1 = xlsread(filename, sheet, x1Range);
CntlPoint_L1 = xml_outL1(:,1);
MU_L1=  xml_outL1(:,3);
GantryRtn_L1 =  xml_outL1(:,4);
CouchVrt_L1 = xml_outL1(:,5);
CouchLat_L1 = xml_outL1(:,6);
CouchLng_L1 = xml_outL1(:,7);
%%
figure
plot (data.MUEA(:,1), data.CouchLngEA(:,1),'--k'); %expected
hold on
plot(data.MUEA(:,2), data.CouchLngEA(:,2), '--g'); % actual
hold on
plot (MU_L1,CouchLng_L1);%intended
hold off
% xlim([0 700]);
ylim([110 120]);
xlabel('MU');
ylabel('Couch Lng (cm)');
title('Couch Lng Vs MU for Straight Line scar');
legend('expected','actual','intended','Location','NorthEast');
%%
figure
plot(data.MUEA(:,1), data.GantryRtnEA(:,1), 'k'); % expected
hold on
plot(data.MUEA(:,2), data.GantryRtnEA(:,2), 'g'); % actual
hold on
plot(MU_L1, GantryRtn_L1, '--b');
hold off
```

```
ylim([170 190]);
xlabel('MU');
ylabel('Gantry Rtn (degrees)');
title('Gantry Rotation Vs MU for Straight Line scar');
legend('expected','actual','intended','Location','Northeast');
%%
figure
plot(data.MUEA(:,1), data.CouchLatEA(:,1), 'k'); % expected axis
hold on
plot(data.MUEA(:,2), data.CouchLatEA(:,2), 'g'); % actual axis
hold on
plot(MU_L1, CouchLat_L1, '--b'); % intended axis
hold off
xlabel('MU');
ylabel('Couch lateral (cm)');
title('Couch Lateral motion Vs MU for Straight Line scar');
legend('expected','actual','intended','Location','Southeast');
%%
figure
plot(data.MUEA(:,1), data.CouchVrtEA(:,1), 'k'); % expected axis
hold on
plot(data.MUEA(:,2), data.CouchVrtEA(:,2), 'g'); % actual axis
hold on
plot(MU_L1, CouchVrt_L1, '--b'); % intended axis
hold off
ylim([90 110]);
xlabel('MU');
ylabel('Couch Vertical (cm)');
title('Couch Vertical motion Vs MU for Straight Line scar');
legend('expected','actual','intended','Location','Northeast');
%%
%  LINE 2
filename='SAGE-Line2';
sheet = 7;
x1Range = 'B40:H50';
xml_outL2 = xlsread(filename, sheet, x1Range);
CntlPoint_L2 = xml_outL2(:,1);
MU_L2 =  xml_outL2(:,3);
GantryRtn_L2 =  xml_outL2(:,4);
CouchVrt_L2 = xml_outL2(:,5);
CouchLat_L2 = xml_outL2(:,6);
CouchLng_L2 = xml_outL2(:,7);

%%
figure
plot (data.MUEA(:,1), data.CouchLngEA(:,1),'--k'); %expected axis
hold on
plot(data.MUEA(:,2), data.CouchLngEA(:,2), '--g'); % actual axis
hold on
plot (MU_L2,CouchLng_L2);%intended axis
hold off
xlabel('MU');
ylabel('Couch Lng (cm)');
```

```
title('Couch Lng Vs MU for scar Line 2-Diagonal');
legend('expected','actual','intended','Location','SouthEast');
%%
figure
plot(data.MUEA(:,1), data.GantryRtnEA(:,1), 'k'); % expected
hold on
plot(data.MUEA(:,2), data.GantryRtnEA(:,2), 'g'); % actual
hold on
plot(MU_L2, GantryRtn_L2, '--b');
hold off
ylim([170  190]);
xlabel('MU');
ylabel('Gantry Rtn (degrees)');
title('Gantry Rotation Vs MU for scar Line 2-Diagonal');
legend('expected','actual','intended','Location','Northeast');
%%
figure
plot(data.MUEA(:,1), data.CouchLatEA(:,1), 'k'); % expected
hold on
plot(data.MUEA(:,2), data.CouchLatEA(:,2), 'g'); % actual
hold on
plot(MU_L2, CouchLat_L2, '--b');
hold off
xlabel('MU');
ylabel('Couch lateral (cm)');
title('Couch Lateral motion Vs MU for scar Line 2-Diagonal');
legend('expected','actual','intended','Location','Southeast');
%%
figure
plot(data.MUEA(:,1), data.CouchVrtEA(:,1), 'k'); % expected
hold on
plot(data.MUEA(:,2), data.CouchVrtEA(:,2), 'g'); % actual
hold on
plot(MU_L2, CouchVrt_L2, '--b');
hold off
ylim ([90 110]);
xlabel('MU');
ylabel('Couch Vertical (cm)');
title('Couch Vertical motion Vs MU for scar Line 2-Diagonal');
legend('expected','actual','intended','Location','Northeast');
%
SCAR ARC 1
filename='SAGEArc1';
sheet = 7;
x1Range = 'B40:H130';
xml_out1 = xlsread(filename, sheet, x1Range);
CntlPoint_Arc1 = xml_out1(:,1);
MU_Arc1 =  xml_out1(:,3);
GantryRtn_Arc1 =  xml_out1(:,4);
CouchVrt_Arc1 = xml_out1(:,5);
CouchLat_Arc1 = xml_out1(:,6);
CouchLng_Arc1 = xml_out1(:,7);
%%
```

```
figure
plot (data.MUEA(:,1), data.CouchLngEA(:,1),'--k'); % expected axis
hold on
plot(data.MUEA(:,2), data.CouchLngEA(:,2), '--g'); % actual axis
hold on
plot (MU_Arc1,CouchLng_Arc1);% intended axis
hold off
ylim([100 110]);
xlabel('MU');
ylabel('Couch Lng (cm)');
title('Couch Lng Vs MU for arc line scar');
legend('expected','actual','intended','Location','NorthEast');
%%
figure
plot(data.MUEA(:,1), data.GantryRtnEA(:,1), 'k'); % expected axis
hold on
plot(data.MUEA(:,2), data.GantryRtnEA(:,2), 'g'); % actual axis
hold on
plot(MU_Arc1, GantryRtn_Arc1, '--b'); % intended axis
hold off
xlabel('MU');
ylabel('Gantry Rtn (degrees)');
title('Gantry Rotation Vs MU for arc line scar');
legend('expected','actual','intended','Location','Northeast');
%%
figure
plot(data.MUEA(:,1), data.CouchLatEA(:,1), 'k'); % expected axis
hold on
plot(data.MUEA(:,2), data.CouchLatEA(:,2), 'g'); % actual axis
hold on
plot(MU_Arc1, CouchLat_Arc1, '--b'); % intended axis
hold off
xlabel('MU');
ylabel('Couch lateral (cm)');
title('Couch Lateral motion Vs MU for arc line scar');
legend('expected','actual','intended','Location','Northeast');
%%
figure
plot(data.MUEA(:,1), data.CouchVrtEA(:,1), 'k'); % expected axis
hold on
plot(data.MUEA(:,2), data.CouchVrtEA(:,2), 'g'); % actual axis
hold on
plot(MU_Arc1, CouchVrt_Arc1, '--b'); % intended axis
hold off
xlabel('MU');
ylabel('Couch Vertical (cm)');
title('Couch Vertical motion Vs MU for arc line scar');
legend('expected','actual','intended','Location','Northeast');
%
Scar Arc 2 plots
filename='SAGE-Arc2';
sheet = 7;
x1Range = 'B40:H130';
```

```
xml_out2 = xlsread(filename, sheet, x1Range);
CntlPoint_Arc2 = xml_out2(:,1);
MU_Arc2=  xml_out2(:,3);
GantryRtn_Arc2 =  xml_out2(:,4);
CouchVrt_Arc2 = xml_out2(:,5);
CouchLat_Arc2 = xml_out2(:,6);
CouchLng_Arc2 = xml_out2(:,7);
 %%
figure
plot (data.MUEA(:,1), data.CouchLngEA(:,1),'--k'); %expected axis
hold on
plot(data.MUEA(:,2), data.CouchLngEA(:,2), '--g'); % actual axis
hold on
plot (MU_Arc2,CouchLng_Arc2);% intended axis
hold off
xlabel('MU');
ylabel('Couch Lng (cm)');
title('Couch Lng Vs MU for scar arc 2');
legend('expected','actual','intended','Location','SouthEast');
 %%
figure
plot(data.MUEA(:,1), data.GantryRtnEA(:,1), 'k'); % expected axis
hold on
plot(data.MUEA(:,2), data.GantryRtnEA(:,2), 'g'); % actual axis
hold on
plot(MU_Arc2, GantryRtn_Arc2, '--b'); % intended axis
hold off
xlabel('MU');
ylabel('Gantry Rtn (degrees)');
title('Gantry Rotation Vs MU for scar arc 2');
legend('expected','actual','intended','Location','Northeast');
%%
figure
plot(data.MUEA(:,1), data.CouchLatEA(:,1), 'k'); % expected axis
hold on
plot(data.MUEA(:,2), data.CouchLatEA(:,2), 'g'); % actual axis
hold on
plot(MU_Arc2, CouchLat_Arc2, '--b'); % intended axis
hold off
xlabel('MU');
ylabel('Couch lateral (cm)');
title('Couch Lateral motion Vs MU for scar arc 2');
legend('expected','actual','intended','Location','Northeast');
%%
figure
plot(data.MUEA(:,1), data.CouchVrtEA(:,1), 'k'); % expected axis
hold on
plot(data.MUEA(:,2), data.CouchVrtEA(:,2), 'g'); % actual axis
hold on
plot(MU_Arc2, CouchVrt_Arc2, '--b'); % intended axis
hold off
xlabel('MU');
ylabel('Couch Vertical (cm)');
```

```
title('Couch Vertical motion Vs MU for scar arc 2');
legend('expected','actual','intended','Location','Northeast');
%
Scar arc 3 plots
filename='SAGE-Arc3';
sheet = 7;
x1Range = 'B40:H130';
xml_out3 = xlsread(filename, sheet, x1Range);
CntlPoint_Arc3 = xml_out3(:,1);
MU_Arc3=  xml_out3(:,3);
GantryRtn_Arc3 =  xml_out3(:,4);
CouchVrt_Arc3 = xml_out3(:,5);
CouchLat_Arc3 = xml_out3(:,6);
CouchLng_Arc3 = xml_out3(:,7);

%%
figure
plot (data.MUEA(:,1), data.CouchLngEA(:,1),'--k'); %expected axis
hold on
plot(data.MUEA(:,2), data.CouchLngEA(:,2), '--g'); % actual axis
hold on
plot (MU_Arc3,CouchLng_Arc3);% intended axis
hold off
xlabel('MU');
ylabel('Couch Lng (cm)');
title('Couch Lng Vs MU for scar arc 3');
legend('expected','actual','intended','Location','NorthEast');
%%
figure
plot(data.MUEA(:,1), data.GantryRtnEA(:,1), 'k'); % expected axis
hold on
plot(data.MUEA(:,2), data.GantryRtnEA(:,2), 'g'); % actual axis
hold on
plot(MU_Arc3, GantryRtn_Arc3, '--b'); % intended axis
hold off
xlabel('MU');
ylabel('Gantry Rtn (degrees)');
title('Gantry Rotation Vs MU for scar arc 3');
legend('expected','actual','intended','Location','Northeast');
%%
figure
plot(data.MUEA(:,1), data.CouchLatEA(:,1), 'k'); % expected axis
hold on
plot(data.MUEA(:,2), data.CouchLatEA(:,2), 'g'); % actual axis
hold on
plot(MU_Arc3, CouchLat_Arc3, '--b');  % intended axis
hold off
xlabel('MU');
ylabel('Couch lateral (cm)');
title('Couch Lateral motion Vs MU for scar arc 3');
legend('expected','actual','intended','Location','Northeast');
% %%
filename='SAGE-Arc4';
```

```
sheet = 7;
x1Range = 'B40:H130';
xml_out4 = xlsread(filename, sheet, x1Range);
CntlPoint_Arc4 = xml_out4(:,1);
MU_Arc4=  xml_out4(:,3);
GantryRtn_Arc4 =  xml_out4(:,4);
CouchVrt_Arc4 = xml_out4(:,5);
CouchLat_Arc4 = xml_out4(:,6);
CouchLng_Arc4 = xml_out4(:,7);
%%
figure
plot (data.MUEA(:,1), data.CouchLngEA(:,1),'--k'); % expected axis
hold on
plot(data.MUEA(:,2), data.CouchLngEA(:,2), '--g'); % actual axis
hold on
plot (MU_Arc4,CouchLng_Arc4);% intended axis
hold off
xlabel('MU');
ylabel('Couch Lng (cm)');
title('Couch Lng Vs MU for scar arc 4');
legend('expected','actual','intended','Location','East');
%%
figure
plot(data.MUEA(:,1), data.GantryRtnEA(:,1), 'k'); % expected axis
hold on
plot(data.MUEA(:,2), data.GantryRtnEA(:,2), 'g'); % actual axis
hold on
plot(MU_Arc4, GantryRtn_Arc4, '--b'); % intended axis
hold off
xlabel('MU');
ylabel('Gantry Rtn (degrees)');
title('Gantry Rotation Vs MU for scar arc 4');
legend('expected','actual','intended','Location','Northeast');
%%
figure
plot(data.MUEA(:,1), data.CouchLatEA(:,1), 'k'); % expected axis
hold on
plot(data.MUEA(:,2), data.CouchLatEA(:,2), 'g'); % actual axis
hold on
plot(MU_Arc4, CouchLat_Arc4, '--b'); % intended axis
hold off
xlabel('MU');
ylabel('Couch lateral (cm)');
title('Couch Lateral motion Vs MU for scar arc 4');
legend('expected','actual','intended','Location','Northeast');
%%
figure
plot(data.MUEA(:,1), data.CouchVrtEA(:,1), 'k'); % expected axis
hold on
plot(data.MUEA(:,2), data.CouchVrtEA(:,2), 'g'); % actual axis
hold on
plot(MU_Arc4, CouchVrt_Arc4, '--b'); % intended axis
hold off
```

```
xlabel('MU');
ylabel('Couch Vertical (cm)');
title('Couch Vertical motion Vs MU for scar arc 4');
legend('expected','actual','intended','Location','Northeast');
%
Arc 2.2 spiral plots
filename='SAGE-Arc2spiral';
sheet = 7;
x1Range = 'B40:H220';
xml_outsp = xlsread(filename, sheet, x1Range);
CntlPoint_Arcsp = xml_outsp(:,1);
MU_Arcsp=  xml_outsp(:,3);
GantryRtn_Arcsp =  xml_outsp(:,4);
CouchVrt_Arcsp = xml_outsp(:,5);
CouchLat_Arcsp = xml_outsp(:,6);
CouchLng_Arcsp = xml_outsp(:,7);

%%
figure
plot (data.MUEA(:,1), data.CouchLngEA(:,1),'--k'); % expected axis
hold on
plot(data.MUEA(:,2), data.CouchLngEA(:,2), '--g'); % actual axis
hold on
plot (MU_Arcsp,CouchLng_Arcsp);% intended axis
hold off
xlabel('MU');
ylabel('Couch Lng (cm)');
title('Couch Lng Vs MU for scar arc-spiral');
legend('expected','actual','intended','Location','SouthEast');
%%
figure
plot(data.MUEA(:,1), data.GantryRtnEA(:,1), 'k'); % expected axis
hold on
plot(data.MUEA(:,2), data.GantryRtnEA(:,2), 'g'); % actual axis
hold on
plot(MU_Arcsp, GantryRtn_Arcsp, '--b'); % intended axis
hold off
xlabel('MU');
ylabel('Gantry Rtn (degrees)');
title('Gantry Rotation Vs MU for scar arc-spiral');
legend('expected','actual','intended','Location','Southeast');
%%
figure
plot(data.MUEA(:,1), data.CouchLatEA(:,1), 'k'); % expected axis
hold on
plot(data.MUEA(:,2), data.CouchLatEA(:,2), 'g'); % actual axis
hold on
plot(MU_Arcsp, CouchLat_Arcsp, '--b'); % intended axis
hold off
xlabel('MU');
ylabel('Couch lateral (cm)');
title('Couch Lateral motion Vs MU for scar arc-spial');
legend('expected','actual','intended','Location','Southeast');
```

```
%%
figure
plot(data.MUEA(:,1), data.CouchVrtEA(:,1), 'k'); % expected axis
hold on
plot(data.MUEA(:,2), data.CouchVrtEA(:,2), 'g'); % actual axis
hold on
plot(MU_Arcsp, CouchVrt_Arcsp, '--b'); % intended axis
hold off
xlabel('MU');
ylabel('Couch Vertical (cm)');
title('Couch vertical motion Vs MU for scar  spiral arc');
legend('expected','actual','intended','Location','Northeast');
```

Calculation of RMSE.

```
%% Calculating RMSE values for Arc scar.
% Intended mechanical axes values from XML are interpolated to have the
same length
% as actual mechanical axes values from log file.

[header, sub, data] = TrajLogReader_v2();
filename='SAGEArc1';
sheet = 7;
x1Range = 'B40:H130';
xml_out1 = xlsread(filename, sheet, x1Range);
CntlPoint_Arc1 = xml_out1(:,1);
MU_Arc1 =  xml_out1(:,3);
GantryRtn_Arc1 =  xml_out1(:,4);
CouchVrt_Arc1 = xml_out1(:,5);
CouchLat_Arc1 = xml_out1(:,6);
CouchLng_Arc1 = xml_out1(:,7);
%%
figure
plot (data.MUEA(:,1), data.CouchLngEA(:,1),'--k'); % expected axis
hold on
plot(data.MUEA(:,2), data.CouchLngEA(:,2), '--g'); % actual axis
hold on
plot (MU_Arc1,CouchLng_Arc1);% intended axis
hold off
ylim([100 110]);
xlabel('MU');
ylabel('Couch Lng (cm)');
title('Couch Lng Vs MU for arc line scar');
legend('expected','actual','intended','Location','NorthEast');
%%
figure
plot(data.MUEA(:,1), data.GantryRtnEA(:,1), 'k'); % expected axis
hold on
plot(data.MUEA(:,2), data.GantryRtnEA(:,2), 'g'); % actual axis
hold on
plot(MU_Arc1, GantryRtn_Arc1, '--b'); % intended axis
```

```
hold off
xlabel('MU');
ylabel('Gantry Rtn (degrees)');
title('Gantry Rotation Vs MU for arc line scar');
legend('expected','actual','intended','Location','Northeast');
%%
figure
plot(data.MUEA(:,1), data.CouchLatEA(:,1), 'k'); % expected axis
hold on
plot(data.MUEA(:,2), data.CouchLatEA(:,2), 'g'); % actual axis
hold on
plot(MU_Arc1, CouchLat_Arc1, '--b'); % intended axis
hold off
xlabel('MU');
ylabel('Couch lateral (cm)');
title('Couch Lateral motion Vs MU for arc line scar');
legend('expected','actual','intended','Location','Northeast');
%%
figure
plot(data.MUEA(:,1), data.CouchVrtEA(:,1), 'k'); % expected axis
hold on
plot(data.MUEA(:,2), data.CouchVrtEA(:,2), 'g'); % actual axis
hold on
plot(MU_Arc1, CouchVrt_Arc1, '--b'); % intended axis
hold off
xlabel('MU');
ylabel('Couch Vertical (cm)');
title('Couch Vertical motion Vs MU for arc line scar');
legend('expected','actual','intended','Location','Northeast');
%%
% Actual mechanical axes values for Arc scar extracted from trajectory
% log files
ActualMU=data.MUEA(:,2);
ActualGantryAng=data.GantryRtnEA(:,2);
ActualCouchVrt=data.CouchVrtEA(:,2);
ActualCouchLat=data.CouchLatEA(:,2);
ActualCouchLng=data.CouchLngEA(:,2);
%Interpolated(intended) mechanical axes values for Arc scar
x=MU_Arc1;
v= GantryRtn_Arc1;
xq=ActualMU;
Intended_Gtry=interp1(x,v,xq);%Intended Gantry angle axis values from
XML line scar
%%
v1=CouchVrt_Arc1;
Intended_CVrt= interp1(x,v1,xq);%Intended couch vertical axis values
from XML line scar

%%
v2=CouchLat_Arc1;
Intended_Clat = interp1(x,v2,xq);%Intended couch lateral axis values
from XML line scar
```

```
%%
v3=CouchLng_Arc1;
Intended_CLng=interp1(x,v3,xq);%Intended couch longitudinal axis values
from XML line scar
%% RMSE calculation:Formula for obtaining RMSE values.
DiffVrt=(ActualCouchVrt-Intended_CVrt).^2;
B=sum(DiffVrt);
RMSEVrt=sqrt(B/7256); % RMSE value for couch vertical movement
DiffLat=(ActualCouchLat-Intended_Clat).^2;
C=sum(DiffLat);
RMSELat=sqrt(C/7256); % RMSE value for couch lateral movement
DiffLng=(ActualCouchLng-Intended_CLng).^2;
D=sum(DiffLng);
RMSELng=sqrt(D/7256);% RMSE value for couch longitudinal movement
DiffGntryAng=(ActualGantryAng-Intended_Gtry).^2;
E=sum(DiffGntryAng);
RMSEGntryAng=sqrt(E/7256);% RMSE value for gantry rototion
```

```
%% Calculating RMSE values for straight line scar.
% Intended mechanical axes values from XML are interpolated to have the
same length
% as actual mechanical axes values from log file.

[header, sub, data] = TrajLogReader_v2();
filename = 'SAGE-Line1';
sheet = 7;
x1Range = 'B40:H50';
xml_outL1 = xlsread(filename, sheet, x1Range);
CntlPoint_L1 = xml_outL1(:,1);
MU_L1=  xml_outL1(:,3);
GantryRtn_L1 =  xml_outL1(:,4);
CouchVrt_L1 = xml_outL1(:,5);
CouchLat_L1 = xml_outL1(:,6);
CouchLng_L1 = xml_outL1(:,7);
%%
figure
plot (data.MUEA(:,1), data.CouchLngEA(:,1),'--k'); %expected
hold on
plot(data.MUEA(:,2), data.CouchLngEA(:,2), '--g'); % actual
hold on
plot (MU_L1,CouchLng_L1);%intended
hold off
% xlim([0 700]);
ylim([110 120]);
xlabel('MU');
ylabel('Couch Lng (cm)');
title('Couch Lng Vs MU for Straight Line scar');
```

```
legend('expected','actual','intended','Location','NorthEast');
%%
figure
plot(data.MUEA(:,1), data.GantryRtnEA(:,1), 'k'); % expected
hold on
plot(data.MUEA(:,2), data.GantryRtnEA(:,2), 'g'); % actual
hold on
plot(MU_L1, GantryRtn_L1, '--b');
hold off
ylim([170 190]);
xlabel('MU');
ylabel('Gantry Rtn (degrees)');
title('Gantry Rotation Vs MU for Straight Line scar');
legend('expected','actual','intended','Location','Northeast');
%%
figure
plot(data.MUEA(:,1), data.CouchLatEA(:,1), 'k'); % expected axis
hold on
plot(data.MUEA(:,2), data.CouchLatEA(:,2), 'g'); % actual axis
hold on
plot(MU_L1, CouchLat_L1, '--b'); % intended axis
hold off
xlabel('MU');
ylabel('Couch lateral (cm)');
title('Couch Lateral motion Vs MU for Straight Line scar');
legend('expected','actual','intended','Location','Southeast');
%%
figure
plot(data.MUEA(:,1), data.CouchVrtEA(:,1), 'k'); % expected axis
hold on
plot(data.MUEA(:,2), data.CouchVrtEA(:,2), 'g'); % actual axis
hold on
plot(MU_L1, CouchVrt_L1, '--b'); % intended axis
hold off
ylim([90 110]);
xlabel('MU');
ylabel('Couch Vertical (cm)');
title('Couch Vertical motion Vs MU for Straight Line scar');
legend('expected','actual','intended','Location','Northeast');

%%
% Actual mechanical axes values for line scar extracted from trajectory
% log files
ActualMU=data.MUEA(:,2);
ActualGantryAng=data.GantryRtnEA(:,2);
ActualCouchVrt=data.CouchVrtEA(:,2);
ActualCouchLat=data.CouchLatEA(:,2);
ActualCouchLng=data.CouchLngEA(:,2);
%Interpolated(intended) mechanical axes values for line scar
x=MU_L1;
v=GantryRtn_L1;
xq=ActualMU;
```

```
Intended_Gtry=interp1(x,v,xq);%Intended Gantry angle axis values from
XML line scar

%%
v1=CouchVrt_L1;
% xq1= ActualCouchVrt;
Intended_CVrt= interp1(x,v1,xq);%Intended couch vertical axis values
from XML line scar

%%
v2=CouchLat_L1;
% xq2=ActualCouchLat;
Intended_Clat = interp1(x,v2,xq);%Intended couch lateral axis values
from XML line scar

%%
v3=CouchLng_L1;
% xq3=ActualCouchLng;
Intended_CLng=interp1(x,v3,xq);%Intended couch longitudinal axis values
from XML line scar

%% RMSE calculation:Formula for obtaining RMSE values.
DiffVrt=(ActualCouchVrt-Intended_CVrt).^2;
B=sum(DiffVrt);
RMSEVrt=sqrt(B/2315); % RMSE value for couch vertical movement
DiffLat=(ActualCouchLat-Intended_Clat).^2;
C=sum(DiffLat);
RMSELat=sqrt(C/2315); % RMSE value for couch lateral movement
DiffLng=(ActualCouchLng-Intended_CLng).^2;
D=sum(DiffLng);
RMSELng=sqrt(D/2315);% RMSE value for couch longitudinal movement
DiffGntryAng=(Intended_Gtry-ActualGantryAng).^2;
E=sum(DiffGntryAng);
RMSEGntryAng=sqrt(E/2315);% RMSE value for gantry rototion
```

Reading film dose matrix and profiles.

```
%%Dose matrix and dose profiles for Film measurement
%%Loading scanned film dose into matlab code
%%Profiles for Straight and Arc line scars
load('DEAR-2-2016-11-29-Dose.mat')
figure
imagesc(0:30,0:28,im);
xlabel('distance, cm');
ylabel('distance, cm')
ARCdose=(im(2300:3000, 1:3350));
figure
imagesc (0:30,0:7,ARCdose);
title ('Dose distribution for arc line scar');
xlabel('distance, cm');
```

```
ylabel('distance, cm');
figure
LINEdose=(im(1200:2000,  500:3000));
imagesc(0:30, 0:7, LINEdose);
xlabel('distance, cm');
ylabel('distance, cm')
title ('Dose distribution for straight line scar');
%% Arc scar dose profiles
ARCdose=(im(2300:3000, 1:3350));
figure
ycoord1=linspace(-9, 8.4, 3350);
ydose1=ARCdose(351, :);
Relatv_dose=(ydose1/500)*100;
plot(ycoord1,Relatv_dose, 'b+');
title ('Cross-plane dose profile for arc scar');
legend('Film dose profile');
%
xcoord1=linspace(-3, 3.8,701);
xdose1=ARCdose(:,1500);
Relatv_dosew=(xdose1/566.45)*100;
figure
plot(xcoord1,Relatv_dosew,'b+');
title ('In-plane dose profile for arc line scar');
% Dose matrix
figure
LINEdose=(im(1200:2000,  500:3000));
imagesc(0:30, 0:7, LINEdose);
xlabel('distance, cm');
ylabel('distance, cm')
title ('Dose distribution for straight line scar');
% Dose profiles
ycoord=linspace(-5, 5,2501);
ydose = LINEdose(401, :);
Relatv_dose1=(ydose/773.86)*100;
figure;
plot(ycoord, Relatv_dose1, 'b+');
title('Cross-plane profile for straight line scar')
xcoord=linspace(-2.50585, 2.50585, 801);
xdose = LINEdose(:,1250);
figure;
Relatv_dose2=(xdose/771.48)*100;
plot(xcoord,Relatv_dose2);
xlabel('distance, cm');
ylabel('Relative Dose (%)');
title ('In-plane dose profile for straight line scar');
```

Dose profiles for dosimetric analysis Matlab codes.

```
clear all,
clc;
format compact;
%%
%% Read eMC DICOM dose file, output png file
eMCFile = 'C:\Users\Joe\Desktop\Reading dose
profiles\RD.DEAR0001_arc1.dcm';
MatOutFile = 'C:\Users\Joe\Desktop\Reading dose
profiles\Dose_Profiles.m';


% fix depth to get the profile
energy = 6;
prof_depths = [1.3; 2.34; 2.91];

%% Read eMC DICOM file
info = dicominfo(eMCFile);
num_fram = info.NumberOfFrames;
mid_fram = round(num_fram/2);
dose_scaling = info.DoseGridScaling*100; % units of cGy
eMCDoseOut = single(dicomread(eMCFile));
eMCDoseOut = eMCDoseOut * dose_scaling;
eMCDoseOut = squeeze(eMCDoseOut);
eMCDoseOut = permute(eMCDoseOut, [2 3 1]);
% get Pixelspacing (mm)
space = info.PixelSpacing;
frameVector = info.GridFrameOffsetVector/10.0; % change to cm

% get DICOM origin coordinates (mm)
dcm_ori = info.ImagePositionPatient;

% the coordinator order changed to 2,3,1, y and z reversed
eMC_x_sq = [dcm_ori(1):space(1):-dcm_ori(1)+1]/10;
eMC_z_sq = [dcm_ori(2):space(2):-dcm_ori(2)]/10+10;
eMC_y_sq = [dcm_ori(3):2.5:-dcm_ori(3)+3]/10;

eMCnx = numel(eMC_x_sq);
eMCny = numel(eMC_y_sq);
eMCnz = numel(eMC_z_sq);
RangeY_eMC = floor(eMCny/2)-1:floor(eMCny/2)+1;
RangeX_eMC = floor(eMCnx/2)-1:floor(eMCnx/2)+1;

% % extraplate the dose in the voxels along the curve
theta = [180:-2:0];
XZ2D = squeeze(mean(eMCDoseOut(:,RangeY_eMC,:), 2));
YZ2D = squeeze(mean(eMCDoseOut(RangeX_eMC,:,:), 1));
PDD_eMC_z = eMC_z_sq;
PDD_eMC = mean(YZ2D(RangeY_eMC,:));
```

```
norf = [100, 50, 10];
radius= 10;
for i = 1:3
% % find the dose with the unfolded coordinator, unfold in XZ plane
only
    x_uf = (radius - prof_depths(i)) * cosd(theta);
    z_uf = radius -(radius - prof_depths(i)) * sind(theta);

    crprf_uf= interp2(eMC_z_sq,eMC_x_sq,XZ2D,z_uf,x_uf);
    crprf_sm = smooth(x_uf, crprf_uf, 0.25,'loess');

    inprf_uf= interp2(eMC_z_sq, eMC_y_sq, YZ2D, prof_depths(i),
eMC_y_sq);
    inprf_sm = smooth(eMC_y_sq, inprf_uf, 0.05,'loess');

    % get the mean for the center voxels of R100 for the normalization
    if i == 1
        crprf_max = mean(crprf_sm(RangeX_eMC));
        inprf_max = mean(inprf_sm(RangeY_eMC));
    end

    crprf_center = mean(crprf_sm(RangeX_eMC));
    inprf_center = mean(inprf_sm(RangeY_eMC));

    % normalized to the center value of R100 and randomly
    % normalize R50 to 50% and R10 to 10%
%
    nprof_cr = norf(i) * (crprf_sm/crprf_max)/(crprf_center/crprf_max)
;
    nprof_in = norf(i) * (inprf_sm/inprf_max)/(inprf_center/inprf_max)
;

    PRF_eMC_x{i,1} = x_uf';
    PRF_eMC_x{i,2} = eMC_y_sq'; % y_uf is same as y_sq
    % extraplated profile
    PRF_eMC_y{i,1} = crprf_uf;
    PRF_eMC_y{i,2} = inprf_uf;
    % smoothed profile
    PRF_eMCs_y{i,1} = crprf_sm;
    PRF_eMCs_y{i,2} = inprf_sm;
%     % nomalized profiles
    PRF_eMCn_y{i,1} = nprof_cr;
    PRF_eMCn_y{i,2} = nprof_in;

end

figure
plot(PRF_eMC_x{1,1}, (PRF_eMC_y{1,1}/250)*120 , 'r.');
xlim([-12, 12]);
ylim([0, 120]);
```

```
xlabel('cross-plane distance (cm)');
ylabel('Dose (cGy)');
title('TPS planed X-plane profile for Arc line scar');
figure
plot(PRF_eMC_x{1,2}, (PRF_eMC_y{1,2}/250)*120 , 'r-.');
xlim([-5, 5]);
ylim([0, 120]);
xlabel('in-plane distance (cm)');
ylabel('Dose (cGy)');
title('TPS planed Y-plane profile for Arc line scar');
  %% Read VL MC output file
%% General parameters  standard field, all rest
%% small field(2mm): 6 (6c), 15(15c), (1mm) 16(6c), 115(15c)
Type = 1; % standard field, cylinder phantom
num_vox_VL=[88,240,88];
RangeX_VL = num_vox_VL(1)/2-2:num_vox_VL(1)/2+2;
RangeY_VL = num_vox_VL(2)/2-2:num_vox_VL(2)/2+2;
GridSize_VL =[0.25, 0.25, 0.25];

% VirtuLinac Simulation input
fullpath_VL = 'C:\Users\Joe\Desktop\Reading dose
profiles\TB6e6c3x3_cylinder11_arc1new_CTcoord2.dose';
MatOutFile = 'C:\Users\Joe\Desktop\Reading dose
profiles\Dose_Profiles.m';

%prof_depths = [1.3 2.34 2.91; 2.1 3.57 4.3; 2.7 5.01 6.04; 2.9 6.60
8.0; 2.5 8.3 10.25];
prof_depths = [1.3; 2.34; 2.91];

%% Read VirtuaLinac output files
[x_sq,y_sq,z_sq,dose_sq] =
VirtuaLinacDoseReader_cylinder(fullpath_VL,Type);

% extraplate the dose in the voxels along the curve
theta = [180:-2:0];
XZ2D = squeeze(mean(dose_sq(:,RangeY_VL,:), 2));
YZ2D = squeeze(mean(dose_sq(RangeX_VL,:,:), 1));
PDD_uf_z = z_sq;
PDD_uf = mean(YZ2D(RangeY_VL,:));

norf = [100, 50, 10];
% find the dose with the unfolded coordinator, unfold in XZ plane only
for i = 1:3
    x_uf = (11 - prof_depths(i)) * cosd(theta);
    z_uf = 11-(11 - prof_depths(i)) * sind(theta);
    crprf_uf= interp2(z_sq,x_sq,XZ2D,z_uf,x_uf);
    crprf_sm = smooth(x_uf, crprf_uf, 0.25,'loess');

    inprf_uf= interp2(z_sq, y_sq, YZ2D, prof_depths(i), y_sq);
    inprf_sm = smooth(y_sq, inprf_uf, 0.05,'loess');
```

```
    % get the mean for the center voxels of R100 for the normalization

    crprf_center = mean(crprf_sm(RangeX_VL));
    inprf_center = mean(inprf_sm(RangeY_VL));

    % normalized to the center value of R100 and randomly
    % normalize R50 to 50% and R10 to 10%

    nprof_cr = norf(i) * (crprf_sm/crprf_center) ;
    nprof_in = norf(i) * (inprf_sm/inprf_center)  ;

    PRF_uf_x{i,1} = x_uf';
    PRF_uf_x{i,2} = y_sq'; % y_uf is same as y_sq
    % extraplated profile
    PRF_uf_y{i,1} = crprf_uf;
    PRF_uf_y{i,2} = inprf_uf;
    % smoothed profile
    PRF_ufs_y{i,1} = crprf_sm;
    PRF_ufs_y{i,2} = inprf_sm;
    % nomalized profiles
    PRF_ufn_y{i,1} = nprof_cr;
    PRF_ufn_y{i,2} = nprof_in;
end

figure
plot(PRF_uf_x{1,1}, PRF_ufn_y{1,1}, 'r');
xlim([-12, 12]);
ylim([0, 140]);
xlabel('cross-plane distance (cm)');
ylabel('Relative Dose (%)');
title('Virtual Linac simulated X-plane profile for Arc line scar');

figure
plot(PRF_uf_x{1,2}, PRF_ufn_y{1,2}, 'r');
xlim([-12, 12]);
ylim([0, 140]);
xlabel('in-plane distance (cm)');
ylabel('Relative Dose (%)');
title('Virtual Linac simulated Y-plane profile for Arc line scar');

%% Reading Virtual Linac output files to plot the cross plane and in-
plane profiles for straight line scar
%% Read VL MC output file
%% General parameters  standard field, all rest
%% small field(2mm): 6 (6c), 15(15c), (1mm) 16(6c), 115(15c)
num_vox_VL=[80,80,75];
RangeX_VL = num_vox_VL(1)/2-1:num_vox_VL(1)/2+1;
RangeY_VL = num_vox_VL(2)/2-1:num_vox_VL(2)/2+1;
GridSize_VL =[0.5, 0.5, 0.2];
%% VirtuLinac Simulation input
```

```
fullpath_VL = 'C:\Users\Joe\Desktop\Reading dose
profiles\TB6e6c3x3_cubic_Line1test4.dose';
MatOutFile = 'C:\Users\Joe\Desktop\Reading dose
profiles\Dose_Profiles.m';
FigOutFile = 'C:\Users\Joe\Desktop\Reading dose
profiles\Dose_Profiles.png';

prof_depths = [1.3 2.34 2.91; 2.1 3.57 4.3;];

%% Read VirtuaLinac output files
[x,y,z,dose] = VirtuaLinacDoseReader_Auto(fullpath_VL, 1,2);

for i = 1:num_vox_VL(3)
    XY2D = dose(RangeX_VL, RangeY_VL,i);
    Depth_VL(i) = mean( mean (XY2D,1), 2);
end

PDD_VL = 100.0*Depth_VL/max(Depth_VL);
DoseMax_VL = max(Depth_VL);

% Analysis - Range
r100 = prof_depths(1);
% r50 = prof_depths(2);
% rp = prof_depths(3)
% define profiles in different depths
prof_z = [r100];


norf = [100];
for i = 1:numel(prof_z)
    [zlayer(i), zlayer(i)] = min( abs(prof_z(i) - z));
    if (prof_z(i) - z(zlayer(i))) > 0
        ceil_layer = zlayer(i) +1;
        floor_layer = zlayer(i);
    else
        ceil_layer = zlayer(i);
        floor_layer = zlayer(i)-1;
    end

    % interplate to the exact z layer between ceilling and floor
    ceil_w = abs(prof_z(i)-z(ceil_layer))/GridSize_VL(3);
    floor_w = abs(prof_z(i)-z(floor_layer))/GridSize_VL(3);
    prof_cr_ceil= mean (dose(:,RangeY_VL,ceil_layer),2 );
    prof_cr_floor= mean (dose(:,RangeY_VL,floor_layer),2 );
    prof_cr = prof_cr_ceil * floor_w + prof_cr_floor*ceil_w;
    prof_in_ceil= mean (dose(RangeX_VL,:,ceil_layer),1);
    prof_in_floor= mean (dose(RangeX_VL,:,floor_layer),1);
    prof_in = prof_in_ceil * floor_w + prof_in_floor*ceil_w;

    % get the mean for the center voxels of R100 for the normalization
    if i == 1
```

```
        crprf_max = mean(prof_cr(RangeX_VL));
        inprf_max = mean(prof_in(RangeY_VL));
    end

        crprf_center = mean(prof_cr(RangeX_VL));
        inprf_center = mean(prof_in(RangeY_VL));

    % normalized to the center value of R100 and randomly
    % normalize R50 to 50% and R10 to 10%
    nprof_cr = norf(i) * (prof_cr/crprf_max)/(crprf_center/crprf_max) ;
    nprof_in = norf(i) * (prof_in/inprf_max)/(inprf_center/inprf_max)
;

    PRF_VL_x{i,1} = x';
    PRF_VL_x{i,2} = y';
    PRF_VL_y{i,1} = nprof_cr;
    PRF_VL_y{i,2} = nprof_in;

end
        figure
        plot(z, PDD_VL,'k.-' );
        xlim([0 6]);
        xlabel('depth (cm)');
        ylabel('Ralative Dose (%)');
        figure
        plot(PRF_VL_x{i,1}, PRF_VL_y{i,1}, 'r.-');
        xlim ([-10 10]);
        xlabel('cross-plane distance (cm)');
        ylabel('Ralative Dose (%)');
        figure
         plot(PRF_VL_x{i,2}, PRF_VL_y{i,2}, 'r.-');
        xlim([-10 10]);
        xlabel('in-plane distance (cm)');
        ylabel('Ralative Dose (%)');
%%
% The plots below show dose profiles for Film measurement, TPS
calculation
% and Virtual Linac Monte Carlo calculation.
%%Loading scanned film dose into matlab code
%Profiles for arc line scar
load('DEAR-2-2016-11-29-Dose.mat')
ARCdose=(im(2300:3000, 1:3350));
figure
ycoord1=linspace(-11, 10.4, 3350);
ydose1=ARCdose(351, :);
Relatv_dose=(ydose1/582.63)*100;
plot(ycoord1,Relatv_dose, 'b+');
hold on;
plot(PRF_eMC_x{1,1}, (PRF_eMC_y{1,1}/250)*120, 'r-.');
hold on;
plot(PRF_uf_x{1,1}, PRF_ufn_y{1,1}, 's-');
hold off;
```

```
xlabel('Central axis distance, cm');
ylabel('Relative Dose (%)');
xlim([-12, 12]);
ylim([0, 120]);
title ('Cross-plane dose profile for arc line scar');
legend('Film dose profile','TPS dose profile','Virtual linac dose
profile','left');
xcoord1=linspace(-3, 3.8,701);
xdose1=ARCdose(:,1500);
Relatv_dosew=(xdose1/566.45)*100;
figure
plot(xcoord1,Relatv_dosew,'b+');
hold on;
plot(PRF_eMC_x{1,2}, ((PRF_eMC_y{1,2}/250)*120) , 'r-.');
hold on;
plot(PRF_uf_x{1,2}, PRF_ufn_y{1,2}, 's-');
hold off;
xlabel('Central axis distance, cm');
ylabel('Relative Dose (%)');
xlim([-5, 5]);
title ('In-plane dose profile for arc line scar');
legend('Film dose profile','TPS dose profile','Virtual linac dose
profile','Northwest');
%%
%% Read eMC DICOM dose file

    eMCFile = 'RD.DEAR0001.dcm';

    %% output file
    FigName = 'Dose_Profiles.png';
    GridSize_eMC = 0.2012;

energy = 6;
prof_depths = 1.3;

    %% Read eMC DICOM file
    eMCDoseOut = single(dicomread(eMCFile));
    info1 = dicominfo(eMCFile);
    space = info1.PixelSpacing;
    frameVector = info1.GridFrameOffsetVector/10.0; % change to cm

    eMC_y = frameVector - info1.NumberOfFrames*0.1  + GridSize_eMC/2.0
-5; % change to cm
    eMC_x = frameVector - double(info1.Columns)*0.1 + GridSize_eMC/2.0
-5; % change to cm

    eMC_z = frameVector-5 + GridSize_eMC/2.0 ; % change to cm
    eMCnx = numel(eMC_x);
    eMCny = numel(eMC_y);
    eMCnz = numel(eMC_z);
```

```
    eMCDoseOut = eMCDoseOut *info1.DoseGridScaling;
    eMCDoseOut = squeeze(eMCDoseOut);
    eMCDoseOut = permute(eMCDoseOut, [2 3 1]);

    RangeY_eMC = floor(eMCny/2)-1:floor(eMCny/2)+1;
    RangeX_eMC = floor(eMCnx/2)-1:floor(eMCnx/2)+1;

    for i = 1:eMCnz;
        XY2D_eMC = eMCDoseOut(RangeX_eMC,RangeY_eMC,i);
        Depth_eMC(i) = mean( mean (XY2D_eMC,1), 2);
    end

    PDD_eMC = 100.0*Depth_eMC/max(Depth_eMC);
    DoseMax_eMC = max(Depth_eMC);
    r100 = prof_depths(1);
    prof_z = r100;
    norf = 100;

    % find the maxium value for cross plane and in plane profile

    for i = 1:numel(prof_z)
        [zlayer(i), zlayer(i)] = min( abs(prof_z(i) - eMC_z));
         if (prof_z(i) - eMC_z(zlayer(i))) > 0
             ceil_layer = zlayer(i) +1;
             floor_layer = zlayer(i);
         else
             ceil_layer = zlayer(i);
             floor_layer = zlayer(i)-1;
         end
         ceil_w = abs(prof_z(i)-eMC_z(ceil_layer))/GridSize_eMC;
         floor_w = abs(prof_z(i)-eMC_z(floor_layer))/GridSize_eMC;
         prof_cr_ceil= mean (eMCDoseOut(:,RangeY_eMC,ceil_layer),2 );
         prof_cr_floor= mean (eMCDoseOut(:,RangeY_eMC,floor_layer),2 );
         prof_cr = prof_cr_ceil * floor_w + prof_cr_floor*ceil_w;
         prof_in_ceil= mean (eMCDoseOut(RangeX_eMC,:,ceil_layer),1);
         prof_in_floor= mean (eMCDoseOut(RangeX_eMC,:,floor_layer),1);
         prof_in = prof_in_ceil * floor_w + prof_in_floor*ceil_w;

         if i == 1
            crprf_max = mean(prof_cr(RangeX_eMC));
            inprf_max = mean(prof_in(RangeY_eMC));
         end

         crprf_center = mean(prof_cr(RangeX_eMC));
         inprf_center = mean(prof_in(RangeY_eMC));

         nprof_cr = norf(i) *
(prof_cr/crprf_max)/(crprf_center/crprf_max) ;
         nprof_in = norf(i) *
(prof_in/inprf_max)/(inprf_center/inprf_max)  ;
```

```
        PRF_eMC_x{i,1} = eMC_x';
        PRF_eMC_x{i,2} = eMC_y';
        PRF_eMC_y{i,1} = nprof_cr;
        PRF_eMC_y{i,2} = nprof_in;

    end

        for i = 1:numel(prof_z)
         figure
            plot(PRF_eMC_x{i,1}, PRF_eMC_y{i,1}, 'b.-');
             xlabel('CAX-distance (cm)');
        ylabel('Ralative Dose (%)');
        legend('Cross-plane profile','Northeast');
        title('TPS planned Line scar dose profiles');
        xlim([-10, 10]);
        ylim([0, 110]);
             figure
            plot(PRF_eMC_x{i,2}, PRF_eMC_y{i,2}, 'y.-');
        xlabel('CAX-distance (cm)');
        ylabel('Ralative Dose (%)');
        legend('In-plane profile','Northeast');
        title('TPS planned Line scar dose profiles');
        xlim([-10, 10]);
        ylim([0, 110]);
        end

%%
%Profiles for straight line scar
% The plots below show dose profiles for Film measurement, TPS
calculation
% and Virtual Linac Monte Carlo calculation.

LINEdose=(im(1200:2000,  500:3000));
ycoord=linspace(-10,11,2501);
ydose = LINEdose(401, :);
xcoord=linspace(-3.7, 3.4, 801);
xdose = LINEdose(:,1251);
Relatv_dose1=(ydose/773.86)*100;
Relatv_dose2=(xdose/771.48)*100;
figure
plot(ycoord, Relatv_dose1, 'b+');
hold on;
plot(PRF_VL_x{i,1}, PRF_VL_y{i,1}, 'g.-');
hold on;
plot(PRF_eMC_x{i,1}, PRF_eMC_y{i,1}, 'r.-');
hold off;
xlabel('Central axis distance, cm');
ylabel('Relative Dose (%)');
legend('Film dose profile','Virtual linac dose profile' ,'TPS dose
profile','Northeast');
xlim([-12 12]);
```

```
ylim([0, 120]);
title ('Cross-plane dose profile for straight line scar');
figure
plot(xcoord,Relatv_dose2, 'b+');
hold on;
plot(PRF_VL_x{i,2}, PRF_VL_y{i,2}, 'g.-');
hold on;
plot(PRF_eMC_x{i,2}, PRF_eMC_y{i,2}, 'r.-');
hold off;
xlabel('Central axis distance, cm');
ylabel('Relative Dose (%)');
xlim([-5 5]);
legend('Film dose profile','Virtual linac dose profile','TPS dose
profile','Northeast');
title ('In-plane dose profile for straight line scar');
```

References

[1] F. M. Khan and J. P. Gibbons, *Khan's the physics of radiation therapy*, Fifth edition. Philadelphia, PA: Lippincott Williams & Wilkins/Wolters Kluwer, 2014.

[2] A. Rodrigues, F.-F. Yin, and Q. Wu, "Dynamic electron arc radiotherapy (DEAR): a feasibility study," *Phys. Med. Biol.*, vol. 59, no. 2, pp. 327–345, Jan. 2014.

[3] A. E. Rodrigues, "Dynamic Electron Arc Radiotherapy (DEAR): A New Conformal Electron Therapy Technique," 2015.

[4] K. R. Hogstrom and P. R. Almond, "Review of electron beam therapy physics," *Phys. Med. Biol.*, vol. 51, no. 13, pp. R455–R489, Jul. 2006.

[5] R. Murthy, H. Gupta, R. Krishnatry, and S. Laskar, "Electron beam radiotherapy for the management of recurrent extensive ocular surface squamous neoplasia with orbital extension," *Indian J. Ophthalmol.*, vol. 63, no. 8, pp. 672–674, Aug. 2015.

[6] S. T. Sonis, "Mucositis: The impact, biology and therapeutic opportunities of oral mucositis," *Oral Oncol.*, vol. 45, no. 12, pp. 1015–1020, Dec. 2009.

[7] H. Mosalaei, S. Karnas, S. Shah, S. Van Doodewaard, T. Foster, and J. Chen, "The use of intensity-modulated radiation therapy photon beams for improving the dose uniformity of electron beams shaped with MLC," *Med. Dosim. Off. J. Am. Assoc. Med. Dosim.*, vol. 37, no. 1, pp. 76–83, 2012.

[8] H. A. Alkhatib *et al.*, "Output calculation of electron therapy at extended SSD using an improved LBR method," *Med. Phys.*, vol. 42, no. 2, pp. 735–740, Feb. 2015.

[9] P. K. Sharma *et al.*, "Electron Arc Therapy for Bilateral Chest Wall Irradiation: Treatment Planning and Dosimetric Study," *Clin. Oncol.*, vol. 23, no. 3, pp. 216–222, Apr. 2011.

[10] A. Rodríguez-Caballero, D. Torres-Lagares, M. Robles-García, J. Pachón-Ibáñez, D. González-Padilla, and J. L. Gutiérrez-Pérez, "Cancer treatment-induced oral mucositis: a critical review," *Int. J. Oral Maxillofac. Surg.*, vol. 41, no. 2, pp. 225–238, Feb. 2012.

[11] M.-J. Kim, S.-H. Park, S.-H. Son, K.-S. Cheon, B.-O. Choi, and T.-S. Suh, "Comparison study of the partial-breast irradiation techniques: Dosimetric analysis of three-dimensional conformal radiation therapy, electron beam therapy, and helical tomotherapy depending on various tumor locations," *Med. Dosim.*, vol. 38, no. 3, pp. 327–331, Sep. 2013.

[12] G. Kemikler, "Dosimetric effects of matching 6MV photon and electron fields in the treatment of head and neck cancers," *Radiat. Meas.*, vol. 41, no. 2, pp. 183–188, Feb. 2006.

[13] A. Alexander, E. Soisson, T. Hijal, A. Sarfehnia, and J. Seuntjens, "Comparison of modulated electron radiotherapy to conventional electron boost irradiation and

volumetric modulated photon arc therapy for treatment of tumour bed boost in breast cancer," *Radiother. Oncol.*, vol. 100, no. 2, pp. 253–258, Aug. 2011.
[14] T. Gauer, K. Engel, A. Kiesel, D. Albers, and D. Rades, "Comparison of electron IMRT to helical photon IMRT and conventional photon irradiation for treatment of breast and chest wall tumours," *Radiother. Oncol.*, vol. 94, no. 3, pp. 313–318, Mar. 2010.
[15] H. Mahdavi, K. Jabbari, and M. Roayaei, "Evaluation of various boluses in dose distribution for electron therapy of the chest wall with an inward defect," *J. Med. Phys.*, vol. 41, no. 1, pp. 38–44, Mar. 2016.
[16] D. D. Leavitt, L. Earley, and J. R. Stewart, "Design and production of customized field shaping devices for electron arc therapy," *Med. Dosim. Off. J. Am. Assoc. Med. Dosim.*, vol. 15, no. 1, pp. 25–31, Mar. 1990.
[17] K. R. Kase and B. E. Bjarngard, "Bremsstrahlung dose to patients in rotational electron therapy," *Radiology*, vol. 133, no. 2, pp. 531–532, Nov. 1979.
[18] K. S. Lam, W. C. Lam, M. J. O'Neill, D. J. Lee, and E. Zinreich, "Electron arc therapy: Beam data requirements and treatment planning," *Clin. Radiol.*, vol. 38, no. 4, pp. 379–383, Jul. 1987.
[19] L. M. Peacock, D. D. Leavitt, F. A. Gibbs, and J. R. Stewart, "Electron arc therapy: clinical experience with chest wall irradiation," *Int. J. Radiat. Oncol. Biol. Phys.*, vol. 10, no. 11, pp. 2149–2153, Nov. 1984.
[20] C.-M. Ma, M. Ding, J. S. Li, M. C. Lee, T. Pawlicki, and J. Deng, "A comparative dosimetric study on tangential photon beams, intensity-modulated radiation therapy (IMRT) and modulated electron radiotherapy (MERT) for breast cancer treatment," *Phys. Med. Biol.*, vol. 48, no. 7, p. 909, 2003.
[21] D. K. Gaffney *et al.*, "Electron arc irradiation of the postmastectomy chest wall with CT treatment planning: 20-year experience," *Int. J. Radiat. Oncol.*, vol. 51, no. 4, pp. 994–1001, Nov. 2001.
[22] D. K. Gaffney, C. M. Lee, D. D. Leavitt, D. C. Shrieve, and J. R. Stewart, "Electron arc irradiation of the postmastectomy chest wall in locally recurrent and metastatic breast cancer," *Am. J. Clin. Oncol.*, vol. 26, no. 3, pp. 241–246, Jun. 2003.
[23] S. V. Jamema, P. K. Sharma, S. Laskar, D. D. Deshpande, and S. K. Shrivastava, "Treatment planning comparison of electron arc therapy and photon intensity modulated radiotherapy for Askin's tumor of chest wall," *Radiother. Oncol.*, vol. 84, no. 3, pp. 257–265, Sep. 2007.
[24] J. D. Richert, K. R. Hogstrom, R. S. Fields, K. L. Matthews, and R. A. Boyd, "Improvement of field matching in segmented-field electron conformal therapy using a variable-SCD applicator," *Phys. Med. Biol.*, vol. 52, no. 9, pp. 2459–2481, May 2007.

[25] D. Henzen *et al.*, "Forward treatment planning for modulated electron radiotherapy (MERT) employing Monte Carlo methods," *Med. Phys.*, vol. 41, no. 3, p. 031712, Mar. 2014.
[26] J. A. Kavanaugh, K. R. Hogstrom, C. Chu, R. A. Carver, J. P. Fontenot, and G. Henkelmann, "Delivery confirmation of bolus electron conformal therapy combined with intensity modulated x-ray therapy," *Med. Phys.*, vol. 40, no. 2, p. 021724, Feb. 2013.
[27] A. Alexander, E. Soisson, M.-A. Renaud, and J. Seuntjens, "Direct aperture optimization for FLEC-based MERT and its application in mixed beam radiotherapy," *Med. Phys.*, vol. 39, no. 8, pp. 4820–4831, Aug. 2012.
[28] J. J. Janssen, E. W. Korevaar, L. J. van Battum, P. R. Storchi, and H. Huizenga, "A model to determine the initial phase space of a clinical electron beam from measured beam data," *Phys. Med. Biol.*, vol. 46, no. 2, pp. 269–286, Feb. 2001.
[29] S. Hyödynmaa, A. Gustafsson, and A. Brahme, "Optimization of conformal electron beam therapy using energy- and fluence-modulated beams," *Med. Phys.*, vol. 23, no. 5, pp. 659–666, May 1996.
[30] E. P. Lief, A. Larsson, and J. L. Humm, "Electron dose profile shaping by modulation of a scanning elementary beam," *Med. Phys.*, vol. 23, no. 1, pp. 33–44, Jan. 1996.
[31] A. Eldib, L. Jin, J. Li, and C.-M. C. Ma, "Feasibility of replacing patient specific cutouts with a computer-controlled electron multileaf collimator," *Phys. Med. Biol.*, vol. 58, no. 16, pp. 5653–5672, Aug. 2013.
[32] A. Eldib, L. Jin, J. Li, and C.-M. C. Ma, "Investigation of the clinical potential of scattering foil free electron beams," *Phys. Med. Biol.*, vol. 59, no. 4, p. 819, 2014.
[33] E. E. El-Khatib, J. Scrimger, and B. Murray, "Reduction of the Bremsstrahlung component of clinical electron beams: implications for electron arc therapy and total skin electron irradiation," *Phys. Med. Biol.*, vol. 36, no. 1, p. 111, 1991.
[34] E. E. Klein, D. A. Low, and J. A. Purdy, "Changes in electron beam dosimetry with a new scattering foil-applicator system on a CL2100C," *Int. J. Radiat. Oncol.*, vol. 32, no. 2, pp. 483–490, May 1995.
[35] N. G. Leveson and C. S. Turner, "An investigation of the Therac-25 accidents," *Computer*, vol. 26, no. 7, pp. 18–41, Jul. 1993.